

Department of Biomedical Engineering and Computational
Science

Monitoring sleep and hypercapnia with near-infrared spectroscopy

Jaakko Virtanen



Monitoring sleep and hypercapnia with near-infrared spectroscopy

Jaakko Virtanen

Doctoral dissertation for the degree of Doctor of Science in
Technology to be presented with due permission of the School of
Science for public examination and debate in Auditorium F239a at
the Aalto University School of Science (Espoo, Finland) on the 16th
of September 2011 at 12 noon.

Aalto University
School of Science
Department of Biomedical Engineering and Computational
Science

Supervisor

Prof. Risto Ilmoniemi

Instructor

DSc (Tech) Tommi Noponen

Preliminary examiners

PD Dr. Martin Wolf, University Hospital Zurich, Switzerland

Prof. Risto Myllylä, University of Oulu, Finland

Opponent

Dr. rer. nat. Jens Steinbrink, Charité - Universitätsmedizin Berlin, Germany

Aalto University publication series

DOCTORAL DISSERTATIONS 65/2011

© Jaakko Virtanen

ISBN 978-952-60-4231-2 (pdf)

ISBN 978-952-60-4230-5 (printed)

ISSN-L 1799-4934

ISSN 1799-4942 (pdf)

ISSN 1799-4934 (printed)

Aalto Print

Helsinki 2011

Finland

The dissertation can be read at <http://lib.tkk.fi/Diss/>

Author

Jaakko Virtanen

Name of the doctoral dissertation

Monitoring sleep and hypercapnia with near-infrared spectroscopy

Publisher School of Science

Unit Department of Biomedical Engineering and Computational Science

Series Aalto University publication series DOCTORAL DISSERTATIONS 65/2011

Field of research Optical imaging of tissue

Manuscript submitted 14 June 2011

Manuscript revised 23 August 2011

Date of the defence 16 September 2011

Language English

Monograph

Article dissertation (summary + original articles)

Abstract

Near-infrared spectroscopy (NIRS) is a medical imaging modality that allows non-invasive estimation of tissue oxygenation and hemodynamics. NIRS has great potential in long-term monitoring of regional cerebral circulation due to its unique combination of excellent temporal resolution, safety and suitability for multimodal measurements, and low cost and portability. Such monitoring can provide valuable information on cerebral oxygenation during voluntary or involuntary cessation of breathing, and on slow changes in spontaneous cerebral activity. However, contribution from extracerebral tissue and motion artefacts hinder interpretation of the measured signals.

This thesis presents methodological improvements to NIRS that aid in separating the cerebral and extracerebral waveforms from NIRS signals measured during hypercapnia (elevated blood carbon dioxide level), and in removing motion artefacts that prevent tracking slow hemodynamic changes. It also describes the cerebrovascular and systemic responses to hypercapnia induced by voluntary breath hold, illustrates differences between voluntary breath hold and obstructive sleep apnea (OSA), and characterises spontaneous cerebral hemodynamic activity during different sleep stages.

The results show that extracerebral contribution to NIRS signals during hypercapnia can be greatly reduced in multi-distance measurements with a blind source separation method such as principal component analysis. In some cases, simply maximising the source–detector separation can provide high sensitivity to cerebral changes with minimal extracerebral interference. Evaluation of experimental data and literature allows identifying potentially clinically significant features of the breath hold and OSA responses. Finally, with the aid of a novel motion artefact reduction method, the slow-wave-sleep stage is shown to be characterised by a significant reduction in slow hemodynamic fluctuations compared to light and rapid-eye-movement sleep. This observation complements previous knowledge of the electrophysiological characteristics of slow-wave sleep, and can help in understanding the unique features and functions of different sleep stages.

Keywords near-infrared spectroscopy; monitoring; hemodynamics; sleep; hypercapnia; extracerebral contribution; motion artefact

ISBN (printed) 978-952-60-4230-5

ISBN (pdf) 978-952-60-4231-2

ISSN-L 1799-4934

ISSN (printed) 1799-4934

ISSN (pdf) 1799-4942

Location of publisher Espoo

Location of printing Helsinki

Year 2011

Pages 133

The dissertation can be read at <http://lib.tkk.fi/Diss/>

Tekijä

Jaakko Virtanen

Väitöskirjan nimi

Unen ja hyperkapnian seuranta lähi-infrapunaspektroskopian avulla

Julkaisija Perustieteiden korkeakoulu**Yksikkö** Lääketieteellisen tekniikan ja laskennallisen tieteen laitos**Sarja** Aalto University publication series DOCTORAL DISSERTATIONS 65/2011**Tutkimusala** Kudoksen optinen kuvantaminen**Käsikirjoituksen pvm** 14.06.2011**Korjatun käsikirjoituksen pvm** 23.08.2011**Väitöspäivä** 16.09.2011**Kieli** Englanti **Monografia** **Yhdistelmäväitöskirja (yhteenveto-osa + erillisartikkelit)****Tiivistelmä**

Lähi-infrapunaspektroskopia (NIRS) on lääketieteellinen kuvantamismenetelmä jolla voidaan mitata kudoksen hapetusastetta ja verenvirtausta ei-invasiivisesti. NIRS soveltuu erittäin hyvin paikallisen aivoverenkierron pitkäaikaismonitorointiin, sillä vaadittu laitteisto voidaan toteuttaa edullisesti ja siirrettävässä muodossa, menetelmä on täysin turvallinen mitattavalle sekä mahdollistaa myös monimenetelmämittaukset, ja verenkierron muutoksia pystytään seuraamaan erinomaisella aikaresoluutiolla. Pitkäaikaismonitoroinnilla voidaan tarkkailla aivojen hapensaannin muutoksia esimerkiksi hengityskatkosten aikana, sekä tutkia hitaita muutoksia aivojen spontaanissa toiminnassa. Aivoja ympäröivien pintakudosten verenkierron ja liikeartefaktoiden vaikutus mitattuihin signaaleihin vaikeuttavat kuitenkin tulosten tulkintaa.

Tässä väitöskirjassa kehitetään NIRS-signaalinkäsittelymenetelmiä pinta- ja aivokudosten verenkierron erottamiseen hyperkapnian (veren normaalia korkeampi hiilidioksidipitoisuus) aikana, sekä sellaisten liikeartefaktoiden poistamiseen jotka estävät hitaiden verenkiertomuutosten seuraamisen monitorointisovelluksissa. Menetelmäkehityksen ohella raportoidaan hengityksenpidätyksen aiheuttamia vasteita aivojen ja pintakudoksen verenkierrossa, kuvaillaan hengityksenpidätyksen ja uniapnean aikaisten hengityskatkosten aiheuttamien vasteiden välisiä eroja, sekä esitellään aivojen spontaanin verenkierron eroja eri univaiheissa.

Väitöskirjan tulokset osoittavat, että hyperkapniamittauksissa voidaan selkeästi vähentää pintakudoksen osuutta NIRS-signaalista käyttämällä muuttujien tilastolliseen erotteluun perustuvia menetelmiä kuten pääkomponenttianalyysiä. Joissain tapauksissa myös lähde-detektorietäisyyden maksimointi antaa riittävän herkkyyden aivoverenkierron muutoksille ilman merkittävää pintakudosvaikutusta. Mittaustulosten ja kirjallisuuskatsauksen perusteella tunnistettiin hengityksenpidätyksen ja uniapneavasteista piirteitä, joilla voi olla kliinistä merkitystä näiden vasteiden fysiologisten vaikutusten arvioinnissa. Uutta liikeartefaktoiden poistomenetelmää käyttävissä unimittauksissa havaittiin spontaanien hitaiden verenkiertomuutosten määrän vähenevän syvässä unessa merkittävästi verrattuna muihin univaiheisiin (kevyt ja vilkeuni). Tämä havainto täydentää aiempaa, elektrofysiologisten mittausten avulla kerättyä tietämystä aivojen ja hermoston toiminnasta unen aikana.

Avainsanat Lähi-infrapunaspektroskopia; monitorointi; verenkierto; uni; hyperkapnia; pintakudoksen vaikutus; liikeartefakta

ISBN (painettu) 978-952-60-4230-5**ISBN (pdf)** 978-952-60-4231-2**ISSN-L** 1799-4934**ISSN (painettu)** 1799-4934**ISSN (pdf)** 1799-4942**Julkaisupaikka** Espoo**Painopaikka** Helsinki**Vuosi** 2011**Sivumäärä** 133**Luettavissa verkossa osoitteessa** <http://lib.tkk.fi/Diss/>

Preface

The human mind is a curious thing. The more you focus on a goal, and the harder you work to achieve it, the more difficult it is to savour the moment once you get there. Instead, the mind most inappropriately tends to fixate on new goals, new challenges to conquer. Without moments of reflection we risk spending the entirety of our lives in pursuit, never satisfied with who we are and what we have.

This thesis is the culmination of a ten-year academic career. During this time I have had the privilege of meeting hundreds of interesting, fun, intelligent, and supportive people. I am particularly fortunate to be able to consider so many of them my friends that it is impossible to thank each one individually for the impression and influence they have had on me, both in personal and professional life. Nevertheless, I wish to convey my deepest gratitude to all of them, and especially to my mother for her love and support throughout my life, and for letting me find my own way.

I also wish to thank my instructor, Tommi, and my supervisor, Risto, for their professional support and advice. Preparing a doctoral thesis is very much an apprenticeship, where one constantly learns from the masters of the trade. The capacity for clear and concise expression is one of the most valuable skills I have learned from you. I also appreciate greatly Dr. Martin Wolf and Prof. Risto Myllylä for their evaluation and suggestions for this thesis. I thank Dr. Jens Steinbrink for accepting the opponent's role in my dissertation, and eagerly await our upcoming conversation.

As for my other scientific collaborators – Jussi, Tapani, Juha, Pekka, Kalle, and Tiina – I have learned something new and fascinating about how the world works from each one of you. As scientists, I am sure you appreciate the value of this statement. I have also enjoyed the wonderful company and collaboration of past and present members of the optical imaging group and others in BECS. Ilkka, Hanna, Petri, Atte, Juha,

Lauri, Tuomas, Hanna, and many others – thank you for all these years.

This work would not have been possible without the resources of the BioMag laboratory at Helsinki University Central Hospital. I am therefore deeply grateful to the management and staff of the laboratory for providing me and dozens of other researchers the opportunity to push the boundaries of human knowledge. My appreciation also extends to the Finnish Cultural Foundation, the Instrumentarium Foundation, and the Research Foundation of Helsinki University of Technology for their generous grants which have made this thesis financially possible.

The Guild of Engineering Physics and Mathematics has a questionable tradition of coaxing young, innocent students into hard labour by using the tactics of persuasion, coercion, trickery, drugging (with alcohol), and sometimes press-ganging. What's astonishing about this is that the victims with nary an exception come back craving for more of the same. Although my studies and thesis probably would have been finished much sooner without it, I wouldn't change my years in the Guild for the world. Again, naming all the culprits would require several pages, but you already know who you are.

One of the most important factors in maintaining your sanity during the preparation of a thesis is peer support. Helena, Suski, Riikka, Silja – I don't think that the meaning of 'tätölounas' can be translated into any language, or even expressed in words. And even if it could be, those words would still be too obscene to print here. I'd rather use these few lines to thank Serla for always being there when extraordinary comforting is needed. And Riku – for the past ten years there has been one constant in my life I could always rely on. I have been, and always shall be, your friend. Please keep reminding me of what's important and what's right.

Mirja, Tapio, Laura, Petri, Liisa, Toni, and the rest – it is a wonderful thing to become a member of the family. Babysitting, splitting firewood, and construction work make for great alternatives to somber research. And finally, Juho – your company and love mean more to me than I can say. I can only hope to reciprocate.

Otaniemi, 23rd August 2011,

Jaakko Virtanen

Contents

Preface	v
Contents	vii
List of publications	ix
The Author's contribution	xi
List of symbols and abbreviations	xiii
1 Introduction	1
2 Methodology of NIRS	5
2.1 Near-infrared light in tissue	5
2.2 The modified Beer–Lambert law	6
2.3 NIRS instrumentation	7
2.4 Interpreting NIRS data	10
3 Monitoring setups	13
3.1 Hypercapnia	13
3.2 Sleep	14
4 Removing extracerebral contribution and motion artefacts	19
4.1 Extracerebral contribution and MBL	19
4.1.1 Results and discussion	20
4.2 Extracerebral contribution in OSA and breath hold mea- surements	21
4.2.1 Results and discussion	22
4.3 Motion artefacts	25
4.3.1 Results and discussion	26

5 Cerebral hemodynamics during breath hold	29
5.1 Results and discussion	30
6 Hemodynamics of sleep	33
6.1 Results and discussion	34
7 Conclusions and closing remarks	41
Bibliography	43
Publications	53

List of publications

This thesis consists of an overview and of the following publications which are referred to in the text by their Roman numerals.

I J. Virtanen, T. Nojonen, and P. Meriläinen. Comparison of principal and independent component analysis in removing extracerebral interference from near-infrared spectroscopy signals. *Journal of Biomedical Optics* 14(5), 054032, September/October 2009.

II J. Virtanen, T. Nojonen, K. Kotilahti, J. Virtanen, and R. J. Ilmoniemi. Accelerometer-based method for correcting signal baseline changes caused by motion artifacts in medical near-infrared spectroscopy. *Journal of Biomedical Optics* 16(8), 087005, August 2011.

III J. Virtanen, T. Nojonen, J. Toppila, T. Salmi, and P. Meriläinen. Impaired cerebral vasoreactivity may cause cerebral blood volume dip following obstructive sleep apnea termination. *Sleep and Breathing*, 4 pages, published online in May 2011. DOI 10.1007/s11325-011-0526-9.

IV J. Virtanen, T. Nojonen, and R. J. Ilmoniemi. Properties of end-expiratory breath hold responses measured with near-infrared spectroscopy. In B. J. Tromberg, A. G. Yodh, M. Tamura, E. M. Sevick-Muraca, and R. R. Alfano (editors), *Proceedings of SPIE* 7896, 78960D, 2011.

V T. Näsi, J. Virtanen, T. Nojonen, J. Toppila, T. Salmi, and R. J. Ilmoniemi. Spontaneous hemodynamic oscillations during human sleep and sleep stage transitions characterized with near-infrared spectroscopy. *PLoS ONE*, accepted for publication, 23 pages, August 2011.

The Author's contribution

Publication I: “Comparison of principal and independent component analysis in removing extracerebral interference from near-infrared spectroscopy signals”

In this study, we investigated the efficacy of two signal processing methods in separating cerebral hemodynamic changes from physiological interference in near-infrared spectroscopy (NIRS) data. I participated in planning the study, designed and implemented the application of the two signal processing methods to NIRS signals, analysed the results, wrote the first draft of the manuscript, and edited the final version based on input from the other authors.

Publication II: “Accelerometer-based method for correcting signal baseline changes caused by motion artifacts in medical near-infrared spectroscopy”

This study introduced a novel method for identifying and removing motion artefacts from NIRS signals. I participated in planning the study, designed and implemented the algorithm, applied it to data, analysed the results, wrote the first draft of the manuscript, and edited the final version based on input from the other authors.

Publication III: “Impaired cerebral vasoreactivity may cause cerebral blood volume dip following obstructive sleep apnea termination”

In Publication III, we compared the cortical hemodynamic response to obstructive sleep apnea in one subject to the corresponding breath hold

response in the same subject and in a control group. I participated in planning the study, carried out the measurements, analysed the data, and wrote the manuscript with the other authors providing comments and suggestions.

Publication IV: “Properties of end-expiratory breath hold responses measured with near-infrared spectroscopy”

In this study, we examined in detail the properties and inter-individual variability of the cerebral hemodynamic response to breath hold. I participated in planning the study, carried out the measurements, analysed the results, and wrote the manuscript with the other authors providing comments and suggestions.

Publication V: “Spontaneous hemodynamic oscillations during human sleep and sleep stage transitions characterized with near-infrared spectroscopy”

In Publication V, we investigated the spontaneous hemodynamic properties of sleep. I participated in planning the study, carried out the measurements, participated in analysing the results, wrote the first draft of the manuscript, and edited the final version based on input from the other authors. Näsi and I share first authorship.

List of symbols and abbreviations

Δ	Change in quantity
$[x]$	Concentration of x
AASM	American Academy of Sleep Medicine
ABAMAR	Accelerometer-based algorithm for baseline motion artefact removal
BP	Blood pressure
CBF	Cerebral blood flow
CBV	Cerebral blood volume
CMRO ₂	Cerebral metabolic rate of oxygen
CSU	Coefficient of spatial uniformity
DPF	Differential path length factor
EEG	Electroencephalography
EMG	Electromyography
EOG	Electrooculography
ETCO ₂	End-tidal CO ₂
fMRI	Functional magnetic resonance imaging
HbO ₂	Oxyhemoglobin
HbR	Deoxyhemoglobin
HbT	Total hemoglobin, $[\text{HbT}] = [\text{HbO}_2] + [\text{HbR}]$
HFO	High-frequency oscillations

HR	Heart rate
ICA	Independent component analysis
LFO	Low-frequency oscillations
LS	Light sleep
MBLL	Modified Beer–Lambert law
MEG	Magnetoencephalography
MEMS	Microelectromechanical system
MSE	Mean squared error
NIR	Near-infrared spectroscopy
NIRS	Near-infrared spectroscopy
NREM	Non-REM (sleep)
OSA	Obstructive sleep apnea
PaCO ₂	Partial pressure of CO ₂ in arterial blood
PCA	Principal component analysis
PET	Positron emission tomography
PPGamp	Peak-to-peak amplitude of pulse oximeter signal
PSD	Power spectral density
PSG	Polysomnography
REM	Rapid-eye-movement (sleep)
SD	Standard deviation
SDS	Source–detector separation
SEM	Standard error of the mean
SNR	Signal-to-noise ratio
SpO ₂	Peripheral arterial oxygen saturation
SWS	Slow-wave sleep
TCD	Transcranial Doppler sonography
VLFO	Very-low-frequency oscillations
W	Wakefulness

1. Introduction

Medical near-infrared spectroscopy (NIRS) is a method for estimating tissue oxygenation and hemodynamics non-invasively from the attenuation changes of near-infrared (NIR, 650–950 nm) light.¹ The typical NIRS setup includes a compact probe secured to the surface of the skin, the actual measurement device housing most of the electronics, and a computer for controlling the device. NIRS is commonly used in research settings for studying spontaneous cerebral hemodynamic activity, to determine the cerebral hemodynamic response to various stimuli and task conditions, and for optical imaging of the brain and breast tissue.^{2–4} NIRS also shows great promise in monitoring cerebral hemodynamics and oxygenation in critical care and the operation room, but routine clinical use for these purposes is not yet widespread.^{5–8}

In many research applications, NIRS complements information obtained with other imaging modalities. For example, electroencephalography (EEG) and magnetoencephalography (MEG) measure the electric and magnetic fields generated by neuronal activity, and can be used to directly quantify the properties of neuronal responses evoked by various cognitive and motor tasks and sensory stimuli. This neuronal activity also leads to an increase in blood flow to the activated cortical region,^{9,10} and NIRS can be used simultaneously with EEG or MEG to study both the neuronal and vascular aspects of the response.^{11,12} However, responses to external stimuli account for only a small portion of the brain's energy consumption.¹³ Various multimodal studies of spontaneous cerebral activity have provided new insights into the functional architecture of the brain and neuronal processes related to learning.^{14–16}

In measuring cerebral hemodynamics, the range of applications for NIRS overlaps with three other methods: functional magnetic resonance imaging (fMRI), positron emission tomography (PET), and transcranial Doppler

sonography (TCD). Compared to these modalities, NIRS provides a unique combination of sub-second temporal resolution, the ability to measure tissue oxygenation, tolerance to small movements of the subject, operator-free measurement, and safety, low cost, and portability of the equipment.² This makes NIRS particularly attractive for monitoring applications. The main disadvantages associated with NIRS are its poor spatial resolution, which is typically of the order of 1 cm in imaging applications, the difficulty of distinguishing cerebral hemodynamic changes from those that occur in extracerebral tissues, and sensitivity to large or sudden movements which may disturb the tissue–optode contact and cause artefacts in the data.^{4,17,18} Poor spatial resolution is a problem primarily in optical imaging, but extracerebral contribution and motion artefacts are relevant issues also in monitoring applications.

The purpose of this thesis is to introduce methodological improvements to monitoring applications of NIRS, and to establish a reference for typical hemodynamic features of sleep and hypercapnia (increased partial pressure of CO₂ in arterial blood (PaCO₂)). As a byproduct of cellular respiration and a potent cerebral vasodilator, CO₂ has an important role in cerebral blood flow (CBF) regulation, particularly in situations where adequate cerebral oxygenation is compromised, such as anaesthesia and obstructive sleep apnea (OSA).^{19,20} An active topic in NIRS monitoring research,^{21–23} OSA is a sleep-related breathing disorder where loss of muscle tone collapses the upper airway, leading to hypercapnia, cerebral hypoxia, and increased risk of various health problems, including cardiovascular disease and stroke.²⁴ OSA is characterised by repetitive apneas during sleep terminated by brief arousals that lead to temporary restoration of muscle tone without conscious awakening.

I will begin by presenting a short summary of the theory and methodology of NIRS in Chapter 2. Chapter 3 discusses in more detail issues related to NIRS monitoring setups, and presents the sleep, hypercapnia, and OSA measurements carried out for this thesis. In Chapter 4, I will review methodological improvements to NIRS that address the problems of extracerebral contribution and motion artefacts in NIRS signals. Chapter 5 provides a comprehensive description of hemodynamic changes during hypercapnia induced by voluntary end-expiratory breath hold.

Advances in multimodal measurement techniques in the recent years have kindled interest in the interaction between spontaneous hemodynamics and neuronal activity during sleep.^{15,16,25} Due to its suitability

for long-term monitoring, NIRS has great potential in accompanying EEG as a standard inclusion in the sleep research setup. In Chapter 6, I will discuss the behaviour of cerebral hemodynamics during sleep, including novel results from our own research. Finally, in Chapter 7, I will summarise the key points from the preceding Chapters and suggest future topics for NIRS-monitoring-based research studies.

Throughout this overview, the plural pronoun 'we' and its inflections are used when referring to the original research efforts carried out for this thesis. With this usage I wish to emphasise the collective nature of scientific research, and particularly acknowledge the contribution of numerous co-workers and volunteer test subjects to the end result.

2. Methodology of NIRS

2.1 Near-infrared light in tissue

The interaction of NIR photons with tissue may be described by two processes: absorption and scattering. Together, they result in attenuation of light intensity that depends on the distance the photons have traversed in tissue and the absorption and scattering properties of the various molecules present.²⁶ Water is the most abundant of these, but it is relatively transparent to light in the NIR range, and its concentration and thus effect on attenuation is typically considered constant. The low or unchanging concentration or weak absorption properties of most other molecules in tissue make also their contribution to light attenuation changes negligible. However, oxy- (HbO₂) and deoxyhemoglobin (HbR) make up around 15 % of blood mass (1 % of total body mass), and their local concentrations change continuously in response to various physiological processes that influence circulation.²⁷ Furthermore, both molecules are strong light absorbers in the NIR range.³⁰ Attenuation changes of NIR light in tissue are thus primarily caused by concentration changes of HbO₂ and HbR ($\Delta[\text{HbO}_2]$ and $\Delta[\text{HbR}]$). Since the absorption spectra of these two molecules differ strongly from each other in the NIR range, it is possible to estimate both $\Delta[\text{HbO}_2]$ and $\Delta[\text{HbR}]$ by simultaneously measuring light attenuation at two or more NIR wavelengths.

At NIR wavelengths, the typical distance photons travel in tissue before undergoing scattering is of the order of 0.1 mm, so light propagation in tissue in NIRS can be modelled as a diffusion process.²⁶ Instead of being absorbed, some of the diffused light exits the tissue at distances of up to several centimetres from the light source (Fig. 2.1). The proportion of photons that have visited cerebral tissue increases with the distance of the point of exit from the light source, so that in practice measuring

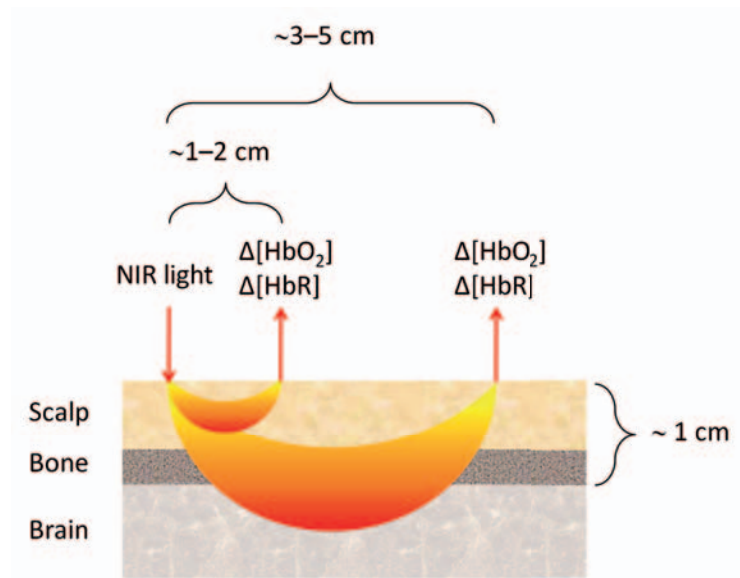


Figure 2.1. A schematic of the principle of NIRS. The arrows indicate points where NIR light is guided into tissue and where light exiting the tissue is detected. The banana-shaped areas indicate the trajectory distribution of the detected photons, with yellow colour indicating high density of the distribution. The contribution of cerebral tissue to the $\Delta[\text{HbO}_2]$ and $\Delta[\text{HbR}]$ estimates increases with the distance from the light source. The distributions are drawn for illustrative purposes only, and are not based on actual simulations.

light attenuation at distances of 3–5 cm from the source allows determining $\Delta[\text{HbO}_2]$ and $\Delta[\text{HbR}]$ in the brain with a good signal-to-noise ratio (SNR).^{28,29} Beyond these distances the number of photons detected is so small that instrumental noise from the measurement electronics starts to dominate, and SNR decreases. Computer simulations of light propagation indicate that the depth of cerebral tissue probed is typically limited to a few millimetres, so NIRS is typically restricted to measuring cortical and subcortical hemodynamic changes.¹⁷

2.2 The modified Beer–Lambert law

Light attenuation in tissue is often modelled in NIRS with the modified Beer–Lambert law (MBLL).²⁶ It is based on the assumption that all attenuation changes are caused by $\Delta[\text{HbO}_2]$ and $\Delta[\text{HbR}]$ in a homogeneous medium, so that scattering and absorption by other chromophores stay

constant. Then the concentration changes are given by

$$\begin{pmatrix} \Delta[\text{HbO}_2] \\ \Delta[\text{HbR}] \end{pmatrix} = \frac{(\alpha^T \alpha)^{-1} \alpha^T}{\text{SDS}} \begin{pmatrix} \Delta A_{\lambda_1} / \text{DPF}_{\lambda_1} \\ \Delta A_{\lambda_2} / \text{DPF}_{\lambda_2} \end{pmatrix}, \quad (2.1)$$

where the 2×2 matrix α contains the specific extinction coefficients for $\Delta[\text{HbO}_2]$ and $\Delta[\text{HbR}]$ at wavelengths λ_1 and λ_2 , and ΔA_{λ_i} is the logarithmic attenuation of light measured with a source–detector separation of SDS from the light source. DPF_{λ_i} is the differential path length factor for λ_i , so that the average path length the detected photons have traversed in tissue is $\text{SDS} \cdot \text{DPF}_{\lambda_i}$. Literature values can be used for both α and DPF ,^{30,31} but some NIRS measurement techniques allow also estimating DPF directly from data (see Section 2.3). MBLL and data-derived DPF values were used in all publications included in this thesis. MBLL also enables estimating concentration changes of other chromophores in tissue such as cytochrome oxidase, a mitochondrial enzyme participating in the cellular respiratory chain.³² However, concentration changes of $\Delta[\text{HbO}_2]$ and $\Delta[\text{HbR}]$ typically dominate in the measured signals, complicating the cytochrome oxidase measurement.

The greatest drawback of MBLL is the assumption of a homogeneous medium, since in reality the light is attenuated in several tissue volumes including skin, muscle, bone, and brain. This partial volume effect means that the measured concentration changes are more accurately interpreted as a weighted average of changes in the individual layers, with the weighting factor depending on the total path length the photons have spent in each tissue and the optical properties of the tissues. In addition to MBLL, several computationally more complex models for light propagation in tissue have been presented. These models are outside the scope of this thesis, but several reviews of the topic are available to the reader.^{4,17,26}

2.3 NIRS instrumentation

Most NIRS instruments are based on one of three core designs: continuous wave, time domain, or frequency domain.²⁶ The designs differ from each other primarily in the manner by which light attenuation and other variables are estimated. Depending on the design and individual device, the light sources and detectors may be integrated into the probe placed on the surface of the skin, or they may be connected to the probe via optical fibres.

The continuous-wave design is the simplest of the three, and is often used in commercial devices due to its ease of implementation, low cost, and compactness.⁵ The continuous-wave method is based on directly measuring light intensity, and only allows measurement of relative changes in hemodynamic parameters. An advanced version of the continuous-wave method, spatially resolved spectroscopy, utilises several closely spaced detectors to correct for the partial volume effect, and allows estimating absolute values of the tissue oxygenation index (TOI).^{33–35}

$$\text{TOI} = \frac{[\text{HbO}_2]}{([\text{HbO}_2] + [\text{HbR}])} \cdot 100\%. \quad (2.2)$$

TOI values derived with spatially resolved spectroscopy have been shown to correlate well with invasively measured cerebral venous oxygen saturation, but their accuracy in absolute quantification varies between commercial devices.^{35,36}

Time domain instruments are based on measuring the time-of-flight distribution of photons in tissue from short (tens of picoseconds) light pulses.^{5,37–39} This enables estimating both light attenuation and DPF directly from data. Unlike continuous-wave and frequency domain instruments, the time domain technique allows screening of photons based on flight time, leading to better depth sensitivity.⁴⁰ High cost and complexity of equipment are the primary obstacles for widespread adoption of time domain technology into clinical use.⁵

The frequency domain method is based on radio frequency (50–1000 MHz) modulation of the light source intensity.^{5,41,42} Amplitude changes of the detected modulation signal are directly proportional to attenuation changes of light in tissue. If also the phase of the detected signal relative to the original signal is determined, the mean path length of photons in tissue can be estimated.⁴³ Frequency domain instruments generally have a good SNR and are technically simpler and less expensive than time domain devices.⁵ Along with time domain devices, they also allow quantifying the absorption and scattering properties of tissue, a prerequisite for diffusion-equation-based models for separating the optical properties of surface and cortical tissues.^{4,17,44}

A frequency domain instrument developed at Aalto University was used in the publications constituting this thesis (Fig. 2.2).^{45,46} It includes four laser diodes at different wavelengths that are coupled to tissue through optical switches based on microelectromechanical system (MEMS) technology and optical fibres. By multiplexing light from different lasers to the optical fibres, up to 16 source positions and four wavelengths can be

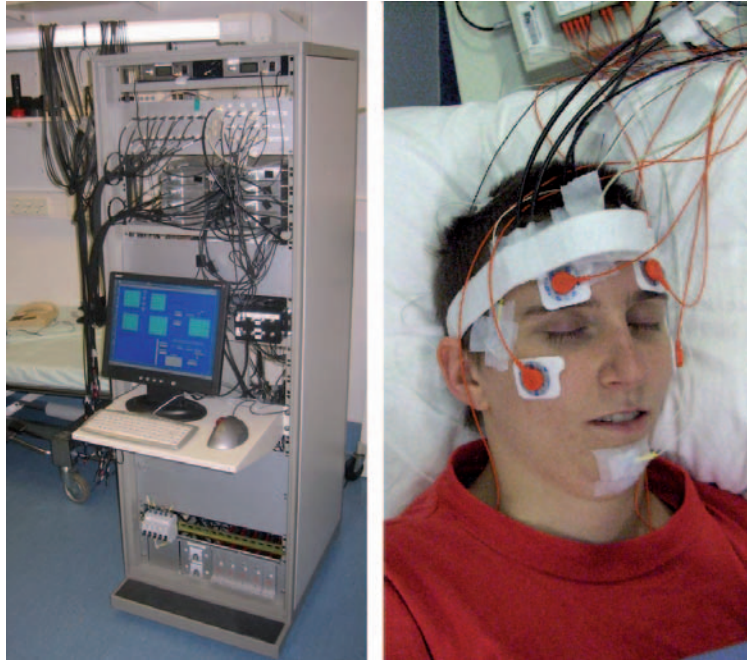


Figure 2.2. The frequency domain instrument used in the measurements (left), and a typical multimodal sleep measurement setup including optical fibres and polysomnography (PSG) electrodes (right).

included in the measurement configuration. Light is detected with 16 photomultiplier tubes coupled to tissue with optical fibre bundles. To estimate the path length of photons in tissue, phase delays introduced to the detected modulation signal by individual source and detector channels have to be eliminated. This is done with a calibration measurement on a polymer resin phantom mimicking the optical properties of tissue.⁴⁶

To facilitate multimodal measurements with, e.g., MEG and transcranial magnetic stimulation, reflecting prism terminals have been developed for coupling the optical fibres into tissue (Fig. 2.3). They allow laying the fibres parallel to the surface of the head, leaving more room for other measurement equipment. Fibres coupled with prism terminals were also used in the sleep and breath hold measurements of Publications II–V to make the subjects more comfortable and to reduce the susceptibility of the tissue–optode coupling to movement.

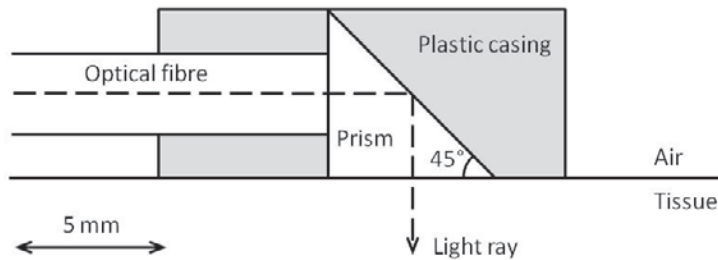


Figure 2.3. A schematic of the prism terminals used when the measurement setup requires the optical fibres to be parallel to surface of the head. (Modified from Publication II.)

2.4 Interpreting NIRS data

The values of $\Delta[\text{HbO}_2]$ and $\Delta[\text{HbR}]$ given by MBLL represent average concentration changes in the whole tissue volume probed. However, hemoglobin in tissue is confined to arteries, capillaries, and veins. If the diameter of the blood vessels increases, both the total amount of blood and the total hemoglobin concentration ($[\text{HbT}] = [\text{HbO}_2] + [\text{HbR}]$) in the tissue volume increase accordingly. Consequently, $\Delta[\text{HbT}]$ is commonly used in NIRS as an indicator of cerebral blood volume (CBV) changes.^{23,28,47,48}

Oxygenated blood is constantly transported to the brain via arteries, displacing deoxygenated blood which is passively drained by the veins. CBF is determined by the difference between the arterial and intracranial pressures and cerebrovascular resistance.⁴⁹ The latter primarily depends on the arterial diameter, which reacts directly to various metabolites related to neuronal activity, such as CO_2 , and is also controlled by a complex and incompletely understood interaction between neurons, glial cells, and vasculature.^{9,50} Increases and decreases in arterial diameter increase and decrease CBF locally in response to stimuli and tasks as well as a part of spontaneous cerebral activity.^{9,14} Venous diameter mostly adapts to the incoming CBF until an equilibrium is reached between the flow and venous compliance.⁵¹ Consequently, since vascular diameter directly determines CBV and can also be seen to correlate with CBF in both the arterial and venous compartments, an increase in $[\text{HbT}]$ measured with NIRS implies also an increase in CBF, particularly if the increase comes from $[\text{HbO}_2]$ alone. This interpretation is supported by evidence of the interdependence of CBF and CBV acquired with other modalities.¹⁹

The interpretation of $\Delta[\text{HbO}_2]$ and $\Delta[\text{HbR}]$ is more complicated. An increase in $[\text{HbO}_2]$ may be caused by an increase in CBF, a decrease in

the cerebral metabolic rate of oxygen (CMRO_2), or an increase in arterial $[\text{HbO}_2]$. Similarly, an increase in $[\text{HbR}]$ may be related to a decrease in CBF (since this also slows down the rate at which deoxygenated blood is transported from the brain), an increase in CMRO_2 , or an increase in arterial $[\text{HbR}]$. Interpretation is further complicated by the possibility of simultaneous influence of all three mechanisms and signal contribution from extracerebral tissue.^{47,52}

In addition to hemodynamic changes, NIRS signals also contain artefacts from light attenuation changes at the tissue–optode coupling. These artefacts are typically caused by hair entering or exiting the tissue–optode space, or motion disturbing the coupling.^{18,53–55} They can appear as transient fluctuations in light attenuation data, complicating the interpretation of cerebral activation measurements, or as permanent attenuation baseline changes that invalidate comparison of $\Delta[\text{HbO}_2]$ and $\Delta[\text{HbR}]$ levels before and after the change. The latter artefact type is particularly problematic in long-term monitoring where movements cannot be completely avoided. Motion and postural changes can also result in the actual displacement of blood, particularly in the venous compartment, which may further hinder signal interpretation.⁵⁶

3. Monitoring setups

NIRS is used for monitoring cerebral hemodynamics in both clinical and research settings. These environments place different demands on the monitoring setup. In clinical monitoring, ease of operation and real-time display of compact, unambiguous information on the condition of the patient are of utmost importance. In a research setting there is often more time for preparing the measurement setup, and data is typically analysed in detail only after the whole measurement series is over. This requires careful planning to anticipate issues that may arise in post-processing and data analysis. Important questions include which physiological parameters are relevant for the phenomenon studied, how should the NIRS optodes be positioned, how to minimise artefacts in the data, etc. The experiences gained research studies also allow developing instrumentation and methodology towards a quick and straightforward application in clinical studies. In this Chapter, I will discuss practical issues pertaining to monitoring setups in sleep and hypercapnia studies with NIRS. Three measurement series used in this thesis are presented as case examples.

3.1 Hypercapnia

Due to its strong cerebral vasodilatory properties, CO₂ is used in NIRS to elicit a response that allows distinguishing between cerebral and extracerebral hemodynamics.^{28,29,57} The role of CO₂ in CBF regulation is also important for NIRS monitoring of conditions where cerebral circulation and oxygenation may be compromised, e.g., OSA and anaesthesia.^{21,23,58}

Hypercapnia can be experimentally induced by breathing CO₂-enriched air (see Case Example I).^{28,29,59} Adjusting the gas mixture of the inhaled air allows controlling PaCO₂, so that the relationship between PaCO₂ and

the hemodynamic response can be studied quantitatively. However, due to the difficulties involved with direct blood gas analysis, end-tidal CO₂ concentration (ETCO₂) is typically used as a substitute for PaCO₂.⁶⁰ In recent years, non-invasive transcutaneous PaCO₂ monitors have also been introduced, although different studies have yielded conflicting results on their accuracy.⁶¹

ETCO₂ can be measured (capnography) with a breathing mask or a nasal cannula connected to a gas analyser. Both methods also allow recording respiratory airflow.^{63–65} In addition to capnography, hemodynamic parameters such as peripheral arterial oxygen saturation (SpO₂) and heart rate (HR) are often measured with a pulse oximeter. Also, continuous blood pressure (BP) may be recorded either invasively using an arterial catheter, or non-invasively based on the volume-clamp method.⁶⁶ The invasive measurement is more accurate, but requires a trained professional and is uncomfortable for the patient. Parameters such as HR and BP can be used to identify and remove the contribution of these variables to NIRS signals in various applications.^{67–69}

The CO₂ breathing method does not fully reproduce the conditions related to voluntary or involuntary cessation of breathing, and the inclusion of CO₂ breathing equipment complicates the measurement setup. Voluntary breath hold is a simple alternative method for achieving hypercapnia that does not require additional instrumentation (Case Example II). The breath hold can be performed at the end of inspiration or expiration. The end-inspiratory approach allows observing the hemodynamic response over an extended period, e.g., for studying differences in vascular CO₂ reactivity between groups.^{70,71} It also allows for both timed and maximal breath holds. End-expiratory breath holds are typically shorter, but they also reduce the total measurement duration, offer better reproducibility, and may be more manageable for subjects suffering from severe respiratory disease.⁷²

3.2 Sleep

Sleep is commonly divided into the physiologically distinct rapid-eye-movement (REM) and non-REM (NREM) phases based on a PSG recording comprising EEG, electromyography (EMG), and electrooculography (EOG). In addition to the REM–NREM divide, the traditionally used Recht-

Case Example I: Hyper- and hypocapnia measurements

In Publication I, we used data collected in a previous NIRS hyper- and hypocapnia study on ten volunteers, one of whom was measured twice.²⁹ The measurement protocol included three 2-min periods of hyper- or hypocapnia separated by 4 min of rest, and PaCO₂ was manipulated by allowing the subjects to breathe CO₂-enriched air (hypercapnia) or hyperventilate (hypocapnia). ETCO₂ was monitored to verify that the deviation from rest level ETCO₂ was similar across the study group. Separate measurements were carried out with mild and moderate hyper- and hypocapnia to compare their impact on cerebral hemodynamics. For details on the measurement protocol and physiological results, see the original study.²⁹

Hypercapnia was expected to increase cerebral arterial diameter and thus lead to an increase in CBF and CBV, while hypocapnia should have an opposite effect.¹⁹ The NIRS probe placed on the forehead had two source and ten detector positions (Fig. 3.1), so that altogether twenty $\Delta[\text{HbO}_2]$ and $\Delta[\text{HbR}]$ signals with 1–5-cm SDSs were recorded. This allowed investigating how the contribution of cerebral tissue depends on SDS. In addition, some of the optodes were in direct contact with the skin while others were raised to a 1.6-mm distance from the surface of the skin to study how signal quality depended on the quality of the contact. Based on the results, a criterion was developed for assessing the quality of the tissue–optode contact.⁶²

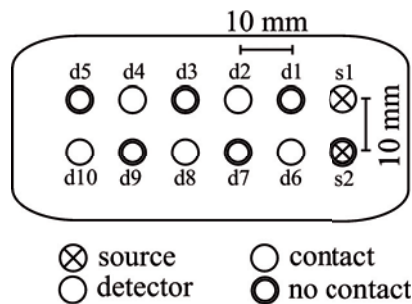


Figure 3.1. The NIRS probe used for the hyper- and hypocapnia measurements. (Modified from Ref. [62].)

Case Example II: Breath hold measurements

In Publication III, eight subjects participated in end-expiratory breath hold measurements designed to mimic the apnea-breathing rhythm associated with OSA. The same data was also used in Publication IV to study the breath hold response in detail. The subjects were instructed to hold their breath after normal expiration for as long as they felt comfortable, and then take a few breaths until they felt comfortable enough to repeat the breath hold. The task was repeated approximately twenty times, and the duration of individual breath holds was approximately 20–40 s, depending on the subject. The subjects laid in a reclining position during the measurement, and the total measurement duration including preparations was approximately one hour.

The NIRS probe was placed on the right side of the forehead and had one source and three detectors at distances of 1, 4, and 5 cm from the source (Fig. 3.2). Based on Publication I, this configuration was deemed to provide the necessary information on local cerebral hemodynamics. The probe was kept in place with a velcro strap wound around the head. A modified S/5 anaesthesia monitor (GE Healthcare Finland Oy, Finland) was used for capnography, spirometry, and pulse oximetry (HR, SpO₂). For capnography and spirometry, the subjects wore a breathing mask covering the nose and mouth (Fig. 3.2).

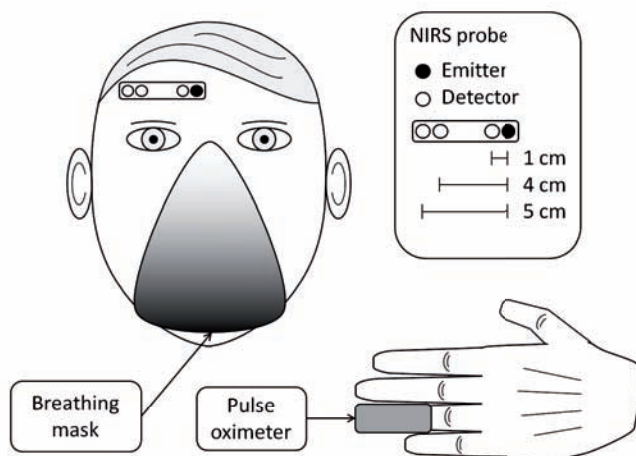


Figure 3.2. The measurement setup for the breath hold measurements. (Modified from Publication IV.)

schaffen–Kales scale for sleep scoring identifies four stages of NREM, S1–S4, and contains separate stages for wakefulness (W) and movement artefacts.⁷³ The Rechtschaffen–Kales scale has recently been superseded by new guidelines from the American Association of Sleep Medicine (AASM), which emphasise the division of NREM into slow-wave (SWS, S3 and S4 in the Rechtschaffen–Kales scale) and light sleep (LS, primarily stages S1 and S2).⁷⁴ There are some other minor differences between the two scoring systems, mostly related to the scoring of transitions between sleep and wakefulness as well as ambiguous and special cases.⁷⁵ In the research presented in this thesis, we mainly followed the rationale behind the AASM guidelines and concentrated on physiological differences between W, LS, SWS, and REM.

The typical sleep monitoring setup will include at least EEG, EOG, and EMG electrodes in order to produce the PSG traces. Also SpO₂, HR, BP, and respiratory airflow or frequency are often recorded, particularly in OSA studies. SpO₂ and HR are derived from the pulsatile component of the pulse oximeter signal, and recent evidence indicates that changes in the peak-to-peak amplitude of the pulsation (PPGamp) may also be used as an indicator of opposite BP changes, albeit with lower accuracy in REM than in NREM sleep.⁷⁶ Patient discomfort with a full breathing mask often limits respiration monitoring to less intrusive means, such as nasal capnography, thermistors, and recording chest movements.^{63,65}

Sleep measurements pose unique challenges for NIRS monitoring (see Case Example III). First of all, the NIRS probe and other measuring equipment must be as comfortable as possible so as not to disturb the quality of sleep. On the other hand, they must also be secured firmly in place since the subject will be moving during sleep. Since rubbing against the pillow can be particularly detrimental to the tissue–optode contact, the placement and configuration of the NIRS probe is often limited to probing the frontal regions of the brain.^{23,77,78} However, more extensive configurations have been used,^{79,80} particularly in short daytime measurements where movement is less of an issue.⁸¹

Case Example III: Sleep measurements

For Publications II and V, 30 all-night NIRS–PSG sleep measurements were conducted on 13 healthy volunteers (Fig. 3.3). In addition, one subject displaying signs of OSA was enrolled for additional sleep measurements including capnography and spirometry (Publication III). In Publications II and V, data from seven nights were discarded partially or completely due to poor EEG contact or the NIRS probe coming off during the night.

The same NIRS probe was used as in the breath hold measurements (Fig. 3.3). The velcro strap attachment was sufficiently robust in most cases, but proved to be unreliable for subjects with long hair. SpO₂, HR, and PPGamp were collected with a fingertip pulse oximeter connected to the S/5 monitor. The monitor was modified to interface with a prototype accelerometer attached to the NIRS probe. The purpose was to record movements which might alter the tissue–optode contact and thus manifest as artefacts in the NIRS data (Publication II). A commercial recorder was used for PSG (Embla A10, Embla Systems, Inc., USA).

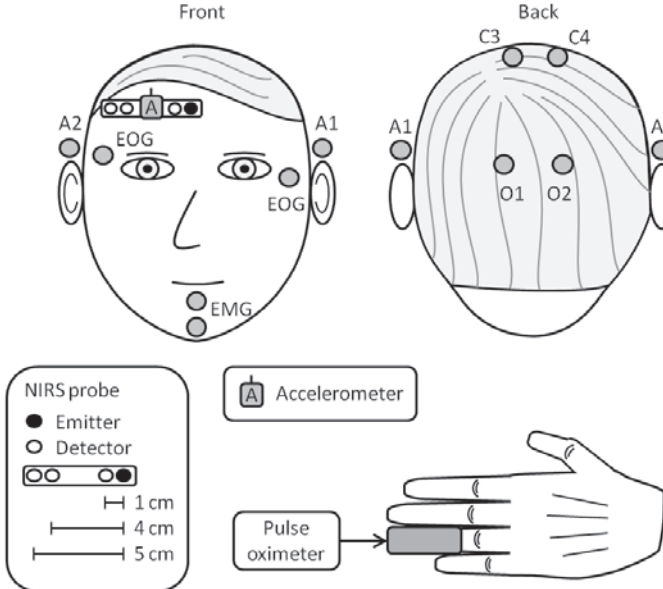


Figure 3.3. The measurement setup for the sleep measurements. EEG electrodes are named according to the international 10–20 system.⁸² x and y refer to the measurement axes of the accelerometer. (Modified from Publication II.)

4. Removing extracerebral contribution and motion artefacts

4.1 Extracerebral contribution and MBLL

In MBLL, the partial volume effect can theoretically be corrected for by estimating the extracerebral $\Delta[\text{HbO}_2]$ and $\Delta[\text{HbR}]$ and subtracting them from the recorded signals to arrive at cerebral $\Delta[\text{HbO}_2]$ and $\Delta[\text{HbR}]$. Depending on the method, this may also require estimating photon path length in different tissues, particularly if quantitative estimates of cerebral changes are desired.² Removal of extracerebral contribution is often based on the assumption that the waveform of the extracerebral signal does not depend on the measurement location.^{69,83,84} This assumption can be considered valid for contribution from systemic hemodynamic variables, i.e., HR, respiratory, and BP fluctuations, although it may not hold in cases where one detector optode is placed directly over a major blood vessel.

Adaptive filtering methods process the NIRS signals with a constantly updating digital filter to minimise similarity to one or more reference signals based on, e.g., a least-mean-squares criterion. The reference signals can include arterial pulsation, HR variability, BP, and blood gas concentrations,^{68,69} but also NIRS signals measured with a short SDS have been used.^{84,85} Adaptive filtering has many advantages for use in clinical monitoring, including computational simplicity and real-time applicability. However, recording several auxiliary signals complicates the measurement setup, and also NIRS signals measured with a short SDS may reflect cerebral hemodynamics depending on the placement of the optodes and individual anatomy. The latter issue is encountered particularly in neonate and infant measurements.

One popular alternative to adaptive filtering are blind source separation methods which make no *a priori* assumptions of the structure of the

data. In particular, principal (PCA) and independent component analyses (ICA) have been applied for extracting cerebral activation signals or removing artefacts from fMRI, EEG, and MEG data.^{86–91} They have also been applied to NIRS data to separate the cerebral and extracerebral waveforms.^{68,83,92–95} The two methods rely on identifying uncorrelated (PCA) or independent (ICA) components in the signals. ICA is statistically more advanced but also more complex, while PCA allows ranking the components based on the variance they explain in the original data. Both methods are primarily suited for removing extracerebral contribution from the complete time series in post-processing, and require that the extracerebral and cerebral signal have different statistical properties.

In Publication I, we compared PCA and ICA in removing extracerebral contribution from the hyper- and hypocapnia data to allow subsequent NIRS studies to make an informed choice between the two. ICA is a non-specific term covering several algorithms, so we chose to use the second-order blind identification algorithm which has been previously applied to NIRS data to detect motor cortex activation.⁶⁸ The previously proposed coefficient of spatial uniformity (CSU) was used for identifying the surface component in ICA.⁸³ In PCA, the component explaining the most variance in the data was removed.

4.1.1 Results and discussion

We found that while both PCA and ICA were capable of removing the extracerebral component from the hyper- and hypocapnia data, PCA performed in most cases better than ICA. Figure 4.1 demonstrates how the mean squared error (MSE) between NIRS signals recorded at SDS = 3 cm and the expected cerebral responses was reduced by treatment with PCA and ICA. The improvement in 3-cm signal quality obtained with PCA was comparable to increasing SDS from 3 to 5 cm, and in some cases even higher. We also varied the number of source–detector combinations included in the analysis from 2 to 20 (cf. Fig. 3.1), and found that the performances of both ICA and PCA generally weakened as the number of signals increased.

The performance differences between PCA and ICA could be in part attributed to the different criteria for choosing the surface component. As the number of signals increases, the number of random-noise components that carry no physiological information also increases. We showed that in

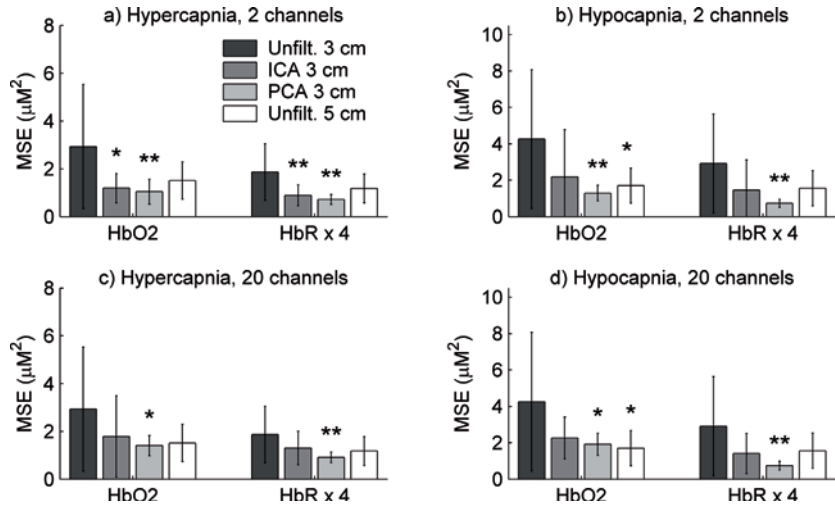


Figure 4.1. The MSE between 3-cm hyper- and hypocapnia signals and the expected response before and after treatment with PCA and ICA. The bars show mean MSE over all subjects, and the error bars show standard deviation (SD) of the mean. The expected response was the average over 5-cm signals recorded from all subjects. The MSE between the individual 5-cm signals and the expected response is shown for reference. Statistically significant difference from the unfiltered 3-cm signals is indicated with * for $p < 0.10$ and with ** for $p < 0.05$. (From Publication I.)

the case of ICA and the CSU criterion, there is a high risk of interpreting one of these random components as extracerebral hemodynamics.

Our comparison of PCA and ICA showed that PCA can be used to improve the sensitivity of NIRS to the cerebral CO₂ response in monitoring applications. This approach is best served by a probe containing one source and two detector positions, with one detector close to the source to record the extracerebral waveform and the other as far away from the source as SNR allows.

4.2 Extracerebral contribution in OSA and breath hold measurements

In Publication III, we compared the cerebral response to OSA-induced hypercapnia with the response to voluntary breath hold simulating OSA. The study was conducted to determine whether OSA-related hemodynamic changes could be explained solely by the influence of hypercapnia on CBF. $\Delta[\text{HbO}_2]$ and $\Delta[\text{HbR}]$ were recorded from one OSA subject and seven controls with 1- and 4-cm SDSs (cf. Figs 3.2 and 3.3). Data from the

5-cm detector was ignored due to poor SNR. Since the apneas elicited a strong extracerebral hemodynamic response, PCA was applied to remove extracerebral contribution from the 4-cm signal. The criterion for the extracerebral component was modified in this study, so that the component that contributed most to the 1-cm signal was removed.

4.2.1 Results and discussion

The 4-cm signals measured from the OSA subject during apnea (Fig. 4.2b) contain a prominent extracerebral component (Fig. 4.2a), while PCA extracts concentration changes that are unique to the brain (Fig. 4.2c). The extracerebral response is characterised by a gradual increase in [HbR] during apnea and a large increase in [HbT] and [HbO₂] following apnea termination, most likely triggered by the associated arousal. The cerebral response (Fig. 4.2c) suggests a decrease in CBV following apnea termination.

Figure 4.3 shows the results of applying PCA to the breath hold data simulating OSA, including breath holds from the OSA subject. In this case, the 4-cm signals do not contain a strong extracerebral component, and applying PCA has almost no perceptible effect on the 4-cm waveforms. Differences in extracerebral contribution to the 4-cm signals between different measurements may be related to the placement of the probe; for example, if the light source is placed directly above a major blood vessel in the scalp, extracerebral hemodynamic changes can be expected to be more prominent in all channels. However, it appears that there are also physiological differences between the OSA and breath hold responses. For example, the scalp response in OSA appears to be exceptionally strong, which could explain why it appears so prominently in the 4-cm signals.

The concentration changes seen in Figs 4.2 and 4.3 are relatively large, especially in the 1-cm signals, considering that the total hemoglobin concentration in tissue should be of the order of 100 μM .²⁷ This may indicate, e.g., systematic underestimation of the 1-cm DPF (cf. Eq. 2.1). Since quantitative interpretation of concentration changes obtained with MBLL is in any case hindered by the partial volume effect, such a systematic error has little impact on the conclusions that can be made from the data. However, it underlines the difficulty of quantitative comparison of $\Delta[\text{HbO}_2]$ and $\Delta[\text{HbR}]$ responses obtained in different study settings.

The results from the OSA and breath hold measurements confirm that

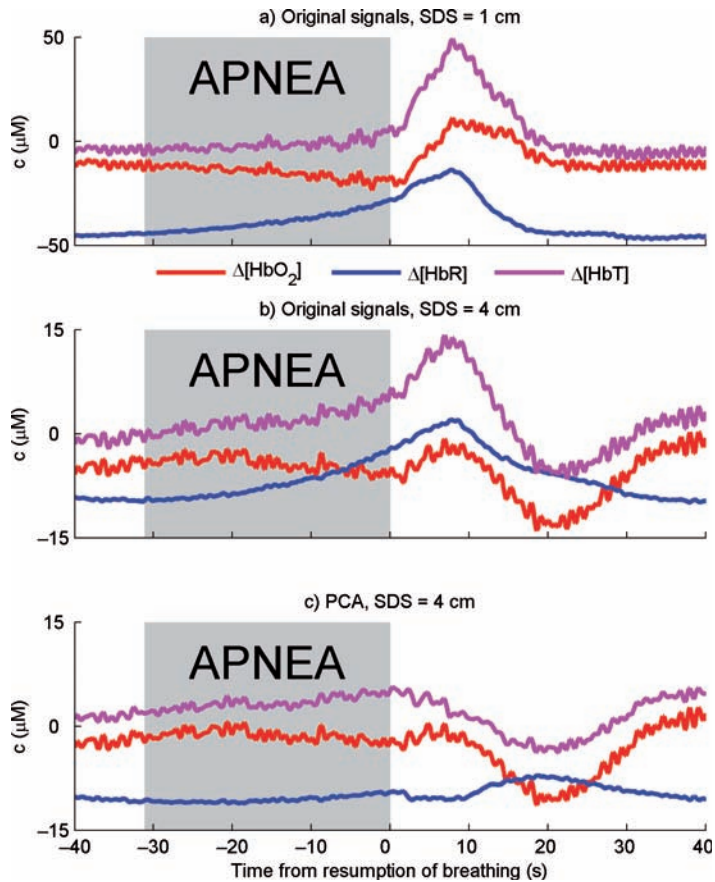


Figure 4.2. Hemoglobin concentration means from 28 apneas with a) 1-cm SDS and b) 4-cm SDS, and c) the 4-cm means after extracerebral contribution has been removed with PCA. Estimated apnea duration is indicated by the grey area. Time 0 s indicates termination of apnea; zero levels for the concentrations have been chosen for visual clarity. A subset of the OSA data presented in Publication III is displayed.

PCA can be used to extract a cerebral waveform that is obscured by extracerebral hemodynamics, but they also demonstrate that a 4-cm signal may in some cases be relatively free of extracerebral contribution, especially when the cerebral response itself is strong and averaged over multiple measurements and subjects. The use of PCA should therefore be guided by visual inspection of the waveforms of NIRS signals recorded at different SDSs to avoid unnecessary signal processing that might lead to artefacts or misinterpretation of data. Furthermore, both the original and PCA-derived waveforms should be taken into account when forming a physiological interpretation of the results. For example, the CBV decrease implied by Fig. 4.2c is also visible in Fig. 4.2b, confirming that the

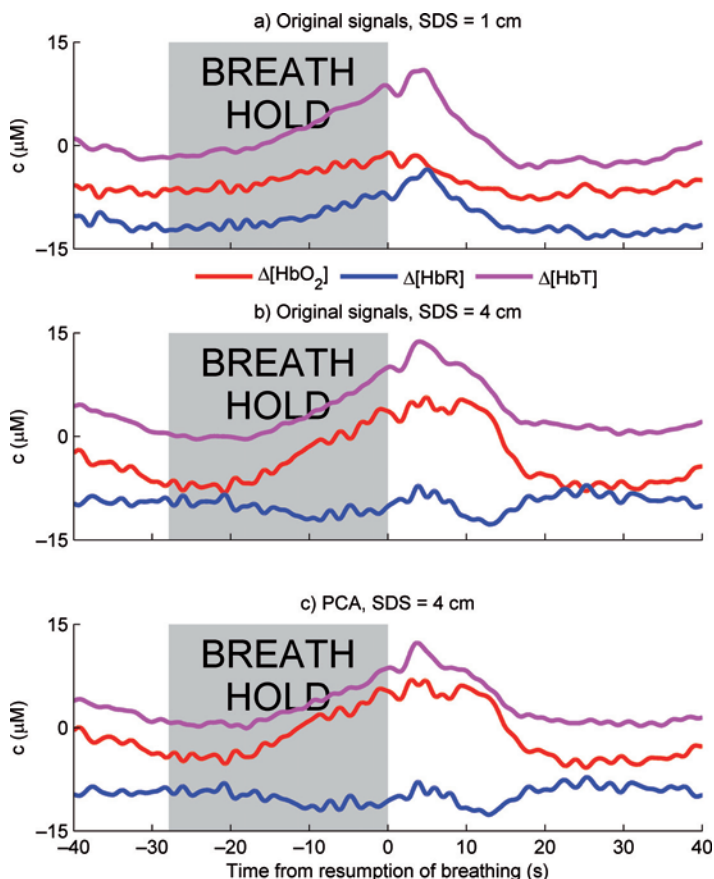


Figure 4.3. Hemoglobin concentration means from 161 breath holds with a) 1-cm SDS and b) 4-cm SDS, and c) the 4-cm means after extracerebral contribution has been removed with PCA.

decrease is not attributable to signal processing artefact and is large compared to other features of the OSA response.

From a physiological point of view, the results indicate a response to OSA different from voluntary hypercapnia, especially since the OSA subject's breath hold response was qualitatively similar to the average response of the control group. Other NIRS OSA studies have not reported CBV decreases following apnea, but only time courses of NIRS signals from individual subjects have been published.^{23,32,96} On the other hand, comparison to TCD measurements supports our observations, suggesting reduced vasoreactivity to PaCO₂ changes during OSA or the arousal event itself as possible explanations for the CBV drop.^{97,98} Since our study was based on a single OSA subject, the results cannot be generalised to the whole OSA population, but they indicate the need to investigate the topic

further.

4.3 Motion artefacts

Both adaptive filtering methods and blind source separation can be used for removing motion artefacts from NIRS signals. Identification of the artefacts is often based on *a priori* assumptions on their statistical properties,^{53–55} or uniformity across different detector channels.¹⁸ Particularly in the latter case, motion artefacts may be implicitly or explicitly considered together with extracerebral hemodynamic contribution under the term global interference.^{84,92,99} Only a few methods have been presented for NIRS motion artefact removal that are based on directly measuring movements of the subject, e.g., with an accelerometer, and they have only been applied to sinusoidal artefacts from nodding and respiration.^{55,100}

In Publication II, we designed and implemented an accelerometer-based algorithm for baseline motion artefact removal (ABAMAR) to allow comparison of $\Delta[\text{HbO}_2]$ and $\Delta[\text{HbR}]$ values before and after periods of motion in long-term monitoring applications such as sleep measurements. ABAMAR can be applied in almost real time, making it also suitable for clinical NIRS monitoring applications, but it does not recover hemodynamic changes or evoked responses that may occur during the motion.

Since no gold standard for NIRS motion artefact identification exists, we validated ABAMAR against visual motion artefact identification by three human classifiers (HC). We also compared artefact detection with ABAMAR to the NIRS-data-based movement artefact reduction algorithm (MARA) presented in.⁵⁴ The MARA algorithm monitors the moving SD of hemoglobin concentrations; if the SD exceeds a preset threshold, a baseline correction is made similar to ABAMAR.

The MARA algorithm also allows recovery of hemodynamic changes during the motion, but this requires *a priori* assumptions about the statistical characteristics of the motion artefact, which is why we chose not to include a similar feature in ABAMAR. Furthermore, recovery of hemodynamic changes during short periods of motion is less relevant in long-term monitoring than in evoked response studies.

4.3.1 Results and discussion

Table 4.1 shows the agreement between ABAMAR and the HCs. The total number of baseline artefacts detected by the HCs varies considerably, but ABAMAR places within this range. From the artefacts identified by ABAMAR, 79 % were identified by at least two HCs (Fig. 4.4). In general, cross-agreement between classifiers depended primarily on the total number of artefacts detected.

Figure 4.5 shows how ABAMAR can in practice influence the interpre-

Table 4.1. The number of artefacts validated between ABAMAR and the HCs. For example, the first row indicates that of the 384 artefacts detected by ABAMAR, 234 were validated by HC1, 304 by HC2, etc. The table is not symmetric around the diagonal since the same event may be registered as one long or several short artefacts by different classifiers.

	Artefacts validated by			
	ABAMAR	HC1	HC2	HC3
ABAMAR	384	234	304	319
HC1	248	324	276	281
HC2	258	295	456	389
HC3	273	338	425	736

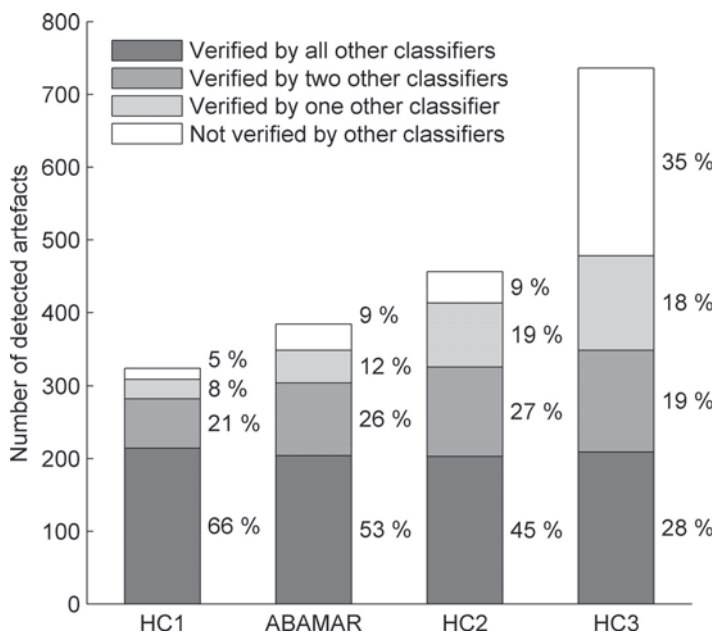


Figure 4.4. Proportion of artefacts confirmed by one, two, or three classifiers for ABAMAR and the three HCs. (From Publication II.)

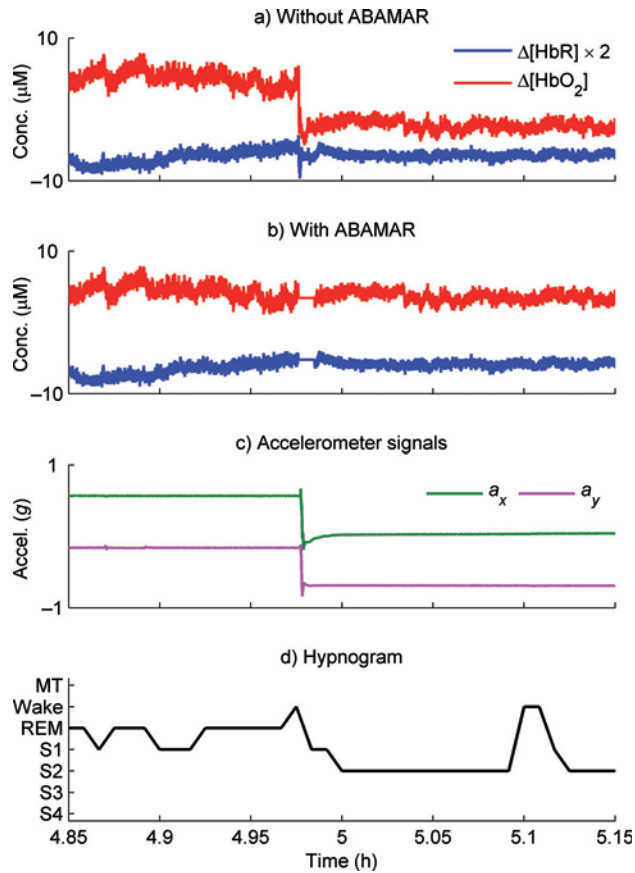


Figure 4.5. a) Hemoglobin concentration changes recorded during sleep with SDS = 4 cm, showing a baseline discontinuity; b) the same signals after processing the data with ABAMAR; c) acceleration along the two accelerometer axes (cf. Fig. 3.3) in units of $g = 9.81 \text{ m/s}^2$, demonstrating movement simultaneously with the baseline discontinuity in a); d) hypnogram showing that the movement was related to a transition from REM to S2 sleep. (From Publication II.)

tation of NIRS data in sleep monitoring. The original data suggests that a transition from REM to S2 sleep is associated with a prominent decrease in $\Delta[\text{HbO}_2]$, but artefact detection and correction with ABAMAR shows that the HbO_2 baseline remains relatively unchanged.

The results shown here and in Publication II demonstrate that ABAMAR can be used to detect and remove baseline motion artefacts from NIRS data with similar accuracy to a human operator. This allows tracking hemodynamic changes over longer time periods than would be otherwise possible in monitoring applications based on the MBLL principle. ABAMAR can also be used in research settings where the study itself requires the subject to move.

Although there was some disagreement between the HCs in artefact detection, it appears that this can be largely attributed to sensitivity to the size of the artefact. In other words, the results can be interpreted so that HC1 marked only large or otherwise unambiguous artefacts, while HC3 marked even relatively ambiguous ones. Comparable levels of disagreement between humans are also seen in sleep scoring,⁷⁵ and requiring at least two HCs to confirm artefacts identified by ABAMAR ensures the reliability of the validation.

Both accelerometer data and artefact identification by the HCs indicated that NIRS data could be expected to contain at least ten baseline artefacts per night. However, analysing the data jointly with MARA and ABAMAR showed that of the ten highest SD peaks in NIRS data per night, more than 20 % were not associated with movement detected by the accelerometer. Thus, the inclusion of an accelerometer into the measurement setup can be seen to improve motion artefact identification compared to purely NIRS-data-based methods.

5. Cerebral hemodynamics during breath hold

The significance of CO₂ to CBF regulation has been acknowledged and studied for decades.^{19,101} Diminished efficiency of the cerebrovascular CO₂ response has been interpreted as an indicator of impaired cerebral autoregulation and incipient vascular endothelial damage that may lead to atherosclerosis and cardiovascular disease.^{97,102} In NIRS breath hold studies, the efficiency of the response has been quantified primarily by $\Delta[\text{HbO}_2]$ and $\Delta[\text{HbR}]$.^{48,71,103} For example, the $\Delta[\text{HbO}_2]$ increase during breath hold has been shown to diminish with age,⁴⁸ and in migraine and OSA patients compared to healthy controls.^{70,104}

Most of these studies have concentrated on the behaviour of $\Delta[\text{HbO}_2]$ and $\Delta[\text{HbR}]$ during breath hold. None of them have described the features of the response in detail, nor have they investigated the variability of the response between different subjects. In particular, differences between cerebral and extracerebral circulation, behaviour of $\Delta[\text{HbR}]$ during breath hold, and the recovery phase after resumption of breathing have not been systematically examined. Thus, it is unclear to what extent the reported $\Delta[\text{HbO}_2]$ responses may be corrupted by extracerebral contribution, which features of the response best quantify its efficiency, and what can be considered normal variation of the response in a healthy population.

In Publication IV, we studied the behaviour of $\Delta[\text{HbO}_2]$, $\Delta[\text{HbR}]$, $\Delta[\text{HbT}]$, HR, and SpO₂ during end-expiratory breath hold in eight healthy volunteers. Our goal was to qualitatively describe the behaviour of these parameters at different phases of the breath hold response, and to quantify the inter- and intraindividual reproducibility of the response. In addition to providing knowledge of the related physiology, this data would aid in designing future breath hold studies.

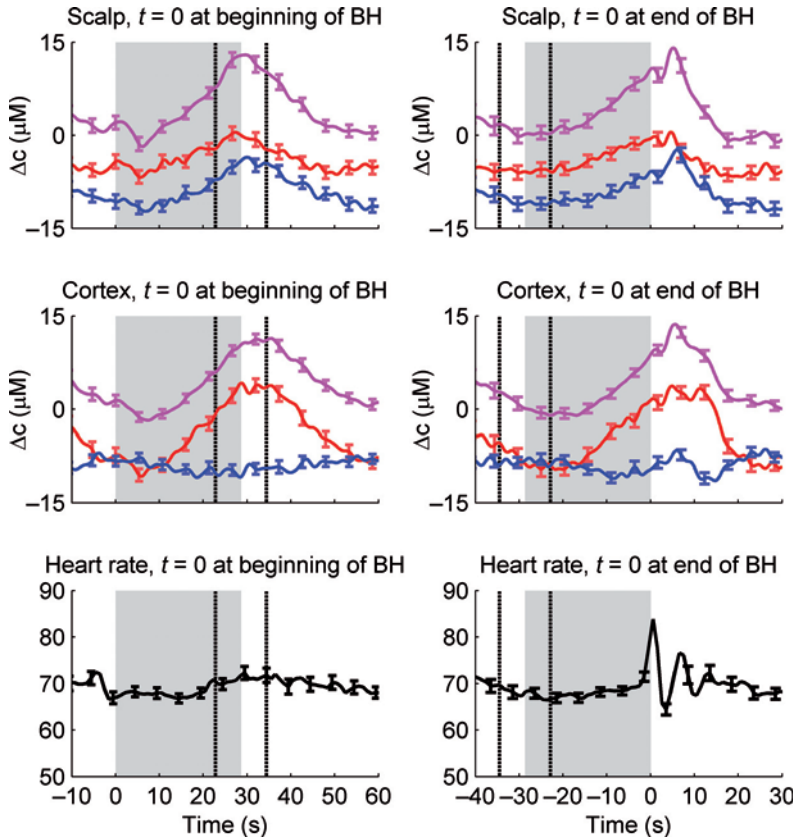


Figure 5.1. Average hemodynamic responses to breath hold (BH) in the study group. $\Delta[\text{HbR}]$, $\Delta[\text{HbO}_2]$, and $\Delta[\text{HbT}]$ are depicted by blue, red, and magenta curves, respectively. Scalp and cortical hemodynamics are given by the 1- and 4-cm detectors, respectively. The grey area indicates average breath hold duration, and the dashed vertical lines its SD. (Modified from Publication IV.)

5.1 Results and discussion

Figure 5.1 shows breath hold responses averaged over the whole study group. Since breath hold duration varied between subjects, the averages have been calculated by aligning the responses first at the beginning of the breath hold and then at breath hold termination. This provides an accurate depiction of both the onset and termination of the response.

As expected, cortical $[\text{HbO}_2]$ increases during the breath hold, while $[\text{HbR}]$ initially decreases due to oxygenated blood replacing deoxygenated blood in the venous compartment. The increasing HbR content of arterial blood is seen first in scalp circulation and slightly later in the cortical signals. Total blood volume clearly increases in both scalp and brain, while HR appears to stay relatively constant during the breath hold. The HR

oscillation after breath hold termination can be attributed to respiration-induced autonomic nervous system modulation of HR.¹⁰⁵ Recovery of all parameters to normal levels occurred within 20–30 s after resumption of breathing, corresponding to subjective readiness to repeat the breath hold task.

A qualitative comparison between individuals reveals a wide range of variance underlying the average response (Table 5.1). For example, HR clearly increases in some individuals but stays level or even decreases in others. A decrease in cortical [HbR] is seen in only three subjects. In fact, the only features common to the whole study group are the increases in cortical [HbO₂] and [HbT] during breath hold. Analysis of the response time courses also showed that only one subject reached maximal vasodilation before the urge to breathe became overwhelming, indicating that end-expiratory breath hold cannot be used to reliably quantify maximal vasodilatory capacity.

Quantitative analysis revealed that the correlation between breath hold duration and the total [HbO₂] increase during breath hold was 0.20. While still statistically significant ($p < 0.05$), the low correlation suggests that Δ [HbO₂] alone is not a good indicator of an individual's CO₂ tolerance. The same applies for the slope of the [HbO₂] increase, which did not correlate statistically significantly with breath hold duration. However, the

Table 5.1. Properties of the breath hold response in individual subjects. Breath hold duration is given as mean \pm standard error of the mean (SEM). The ↗ symbol indicates an increase in the parameter during the breath hold, while ↘ denotes a decrease and — means no perceptible change. The assessments are based on visual interpretation of the signals. HbO₂, HbR, and HbT are abbreviated as O₂, R, and T. The last column gives the average values of the SpO₂ minimum and maximum following each breath hold. (From Publication IV.)

Subject, sex, breath holds	Average duration (s)	Scalp Δ Hb			Cortical Δ Hb			Heart rate	SpO ₂ min / max
		O ₂	R	T	O ₂	R	T		
S5, M, 21	22.5 \pm 0.3	—	—	—	↗	—	↗	—	96.0 / 99.0
S8, M, 18	23.1 \pm 0.7	—	—	—	↗	—	↗	↘	93.2 / 96.7
S4, F, 21	26.5 \pm 0.7	↗	—	↗	↗	↘	↗	—	94.9 / 97.6
S2, M, 19	27.0 \pm 1.0	↗	↗	↗	↗	—	↗	↗	96.1 / 97.8
S7, M, 24	29.2 \pm 0.7	—	↗	↗	↗	↘	↗	↗	92.8 / 97.7
S3, M, 20	29.6 \pm 1.0	↗	↗	↗	↗	—	↗	↗	97.1 / 98.1
S1, M, 18	34.1 \pm 0.4	↗	↗	↗	↗	↘	↗	↗	97.5 / 99.6
S6, M, 20	37.8 \pm 0.7	—	↗	↗	↗	—	↗	↘	96.6 / 98.6

goodness of a linear fit to the $[\text{HbO}_2]$ increase had encouraging measurement repeatability and a relatively good correlation of 0.52 with breath hold duration. This parameter might reflect the stability of CBF during vasodilation, and thereby the efficiency of the response.

In summary, our results enable future breath hold studies to make informed choices on study design: which parameters to monitor, what is the optimal spacing of breath holds, how many subjects and repetitions are required for a given level of measurement reliability, etc. In addition, they provide a qualitative reference for the entire time course of the end-expiratory breath hold response, and illustrate typical variation in the response among normal subjects.

6. Hemodynamics of sleep

Sleep can be described as an alternating sequence of three distinct physiological states: LS, characterised by transient EEG phenomena called spindles and K-complexes; SWS, characterised by EEG delta waves (0–4 Hz); and REM, characterised by complex EEG activity, muscle atonia, and eye movements.⁷⁵ The sleep cycle is thought to be regulated by a variety of homeostatic oscillators, biochemical feedback loops that maintain the operational and adaptive capabilities of an organism on the cellular and systemic levels.^{25,106} Understanding their nature and complex interactions requires studying spontaneous neurophysiological activity over a wide range of time scales. However, technical limitations of conventional EEG and MEG restrict their applicability in studying neuronal oscillations below approximately 0.1 Hz.^{107–109} In addition, EEG and MEG do not reveal changes in spontaneous hemodynamic activity. Therefore, to form a comprehensive understanding of the physiology of sleep, electrophysiological signals must be supplemented with hemodynamic and metabolic monitoring.^{81,110–113}

Previous NIRS studies on sleep hemodynamics have shown that [HbO₂] decreases and [HbR] increases during sleep onset.^{77,78,81} REM sleep has been associated with higher levels of [HbT] and [HbO₂] than NREM sleep.^{77,80} One study has also reported that [HbO₂], [HbR], and [HbT] increase after termination of SWS,⁷⁷ but otherwise SWS has been largely neglected in NIRS studies.

NIRS results are supported by studies with other modalities which indicate a decrease in brain activity in NREM sleep compared to wakefulness.¹⁶ In particular, PET evidence indicates that CBF in NREM sleep correlates negatively with periods of delta activity.¹¹⁴ However, EEG spindles in LS and delta waves in SWS are still associated with local hemodynamic activation compared to the baseline within the sleep stage.^{115,116}

PET studies on REM sleep have demonstrated a level of physiological activity comparable to wakefulness, although there are some differences between brain areas.^{16,117}

Although the baselines of various hemodynamic parameters have been studied extensively in sleep, few studies have attempted to quantify spontaneous hemodynamic fluctuations during sleep. Hemodynamic signals are known to exhibit high-frequency (HFO, 0.15–0.4 Hz), low-frequency (LFO, 0.04–0.15 Hz), and very-low-frequency (VLFO, 0.003–0.04 Hz) oscillations.^{14,105,118–120} Some of these oscillations result from autonomic regulation of BP and HR variability,^{121,122} while others are caused by vasomotion.^{123,124} HR variability in the VLFO and LFO bands was shown to increase from SWS to LS and from LS to REM.¹²⁵ Also cardiac pulsation and respiration are seen as oscillations in NIRS signals.^{118,119} VLFOs and LFOs in cerebral hemodynamics have been shown to predict behavioural responses to task conditions, correlate spatially between brain areas, and aid in research of various pathologies of the brain.^{14,126,127} In addition to true oscillations that are most likely driven by various homeostatic processes, NIRS signals may also contain non-harmonic hemodynamic fluctuations.

In Publication V, we investigated the behaviour of hemodynamic oscillations in W, LS, SWS, and REM by calculating the power spectrum density (PSD) of [HbO₂], [HbR], HR, SpO₂, and PPGamp in the VLFO and LFO bands. We also examined the time evolution of hemodynamic signals in sleep stage transitions, since no previous NIRS study has provided a systematic treatment of this topic. Particular attention was given to SWS, since it has been studied less extensively than LS and REM. The study was also the first effort to extensively quantify and compare spontaneous hemodynamic VLFOs and LFOs in different sleep stages with NIRS.

6.1 Results and discussion

Figures 6.1 and 6.2 demonstrate the behaviour of hemodynamic signals in sleep stage transitions. The data has been averaged over transitions that were preceded and followed by at least 300 s of uninterrupted sleep in the indicated sleep stages. Transitions not involving LS are omitted due to their small number. The results support earlier observations on the behaviour of hemoglobin concentrations during sleep onset and offset,⁷⁸

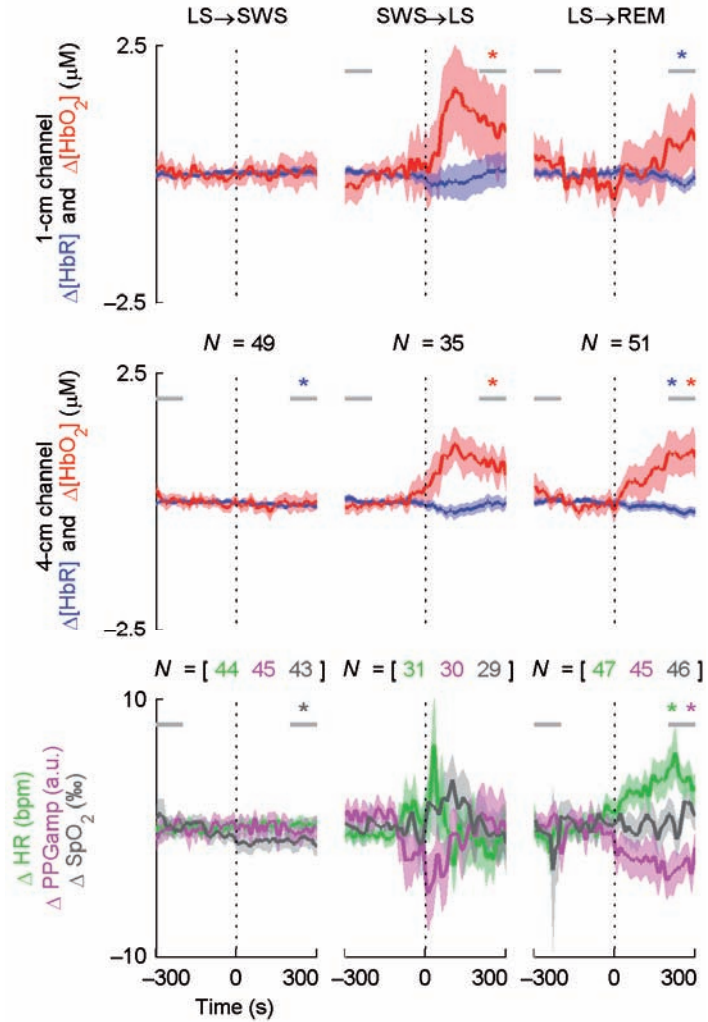


Figure 6.1. Hemodynamic signals in the SWS→LS, LS→SWS, and LS→REM transitions. For each signal, the zero level is the average over $-300 \dots 0$ s. The number of transitions averaged is indicated with N , and the shaded area indicates the 95% confidence interval of the mean. (Modified from Publication V.)

and in the SWS→LS and LS→REM transitions.^{77,80} They also indicate that the latter two hemodynamic transitions are more abrupt than the opposite LS→SWS and REM→LS transitions.

The hemodynamic changes related to the SWS→LS and LS→REM transitions resemble each other greatly, but in the first case the changes are mainly transient, while in the latter they appear to be sustained. This suggests that the changes in the LS→REM transition reflect increased physiological activity in REM sleep, while the changes in the SWS→LS

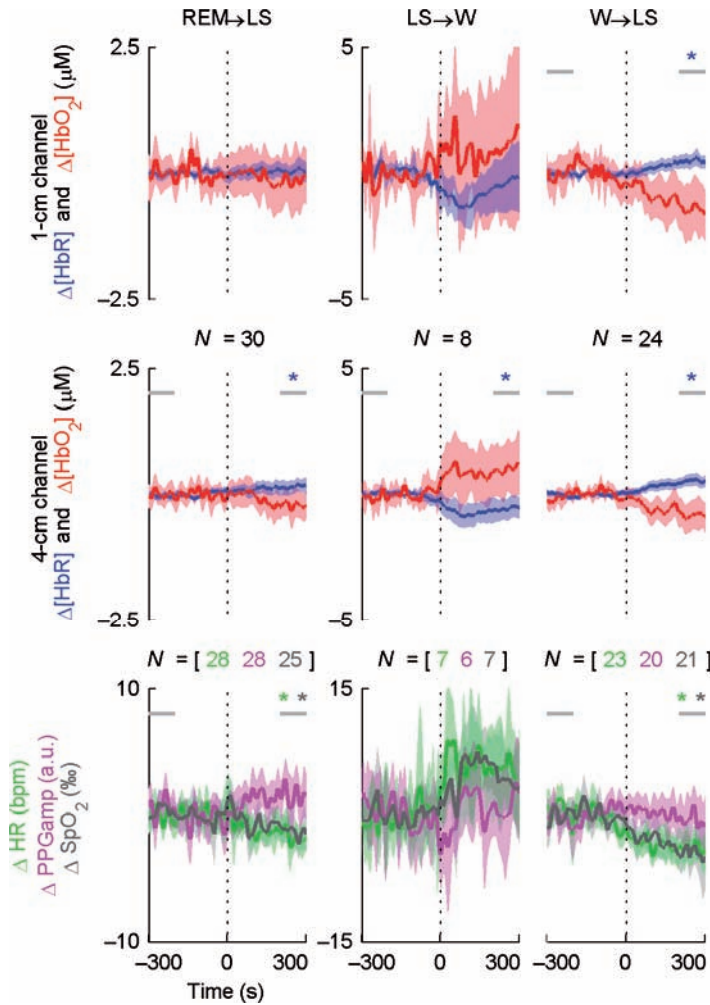


Figure 6.2. Hemodynamic signals in the REM→LS, LS→W, and W→LS transitions. (Modified from Publication V.)

transition are more closely related to the transition itself. For example, the termination of SWS was often accompanied by movement or an arousal, and the hemodynamic changes in the SWS→LS and LS→W transitions resemble each other closely. Therefore, a process similar to awakening might be responsible for the termination of SWS.

The PSD analysis shows that spontaneous hemodynamic oscillations are subdued in SWS compared to other sleep stages in both systemic and cerebral circulation (Fig. 6.3). In contrast, there are almost no differences between LS and REM. These observations can be compared to the previously reported results for HR variability, where the largest differences were seen between NREM and REM.¹²⁵

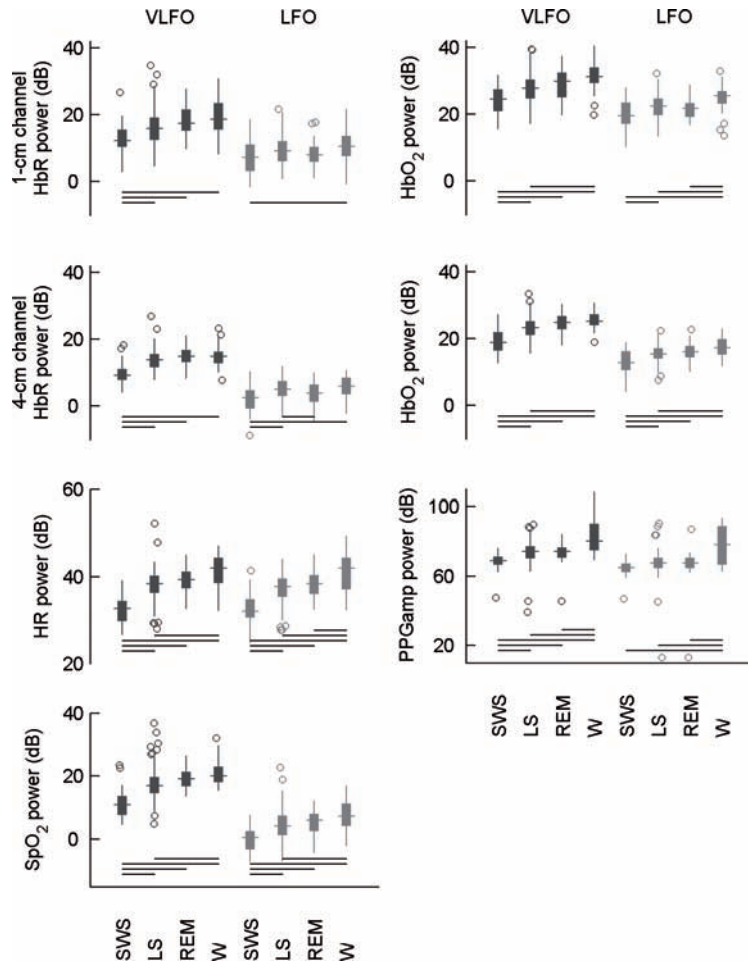


Figure 6.3. The logarithm of signal power in the VLFO and LFO bands for NIRS data and the systemic parameters in different sleep stages. For each stage, the box plot gives the distribution of power in separate periods of SWS, LS, REM, and W. The box corresponds to the interquartile range (IQR) of the distribution, and the horizontal line crossing the box marks the median. The whiskers indicate values that fall within 1.5 IQR of the box, and any remaining outliers are marked with circles. The horizontal lines show which sleep stages differ from each other statistically significantly. (From Publication V.)

The EEG delta waves in SWS result from the synchronous oscillation of neurons over the local brain area.¹²⁸ This behaviour is unique to SWS, and it has been suggested to reflect homeostatic regulation and recalibration of synaptic strengths after their potentiation in periods of learning during wakefulness.¹⁵ A reduction in cerebral hemodynamic oscillations in SWS could reflect reduced CBF variation in the local cortical area because of the neuronal synchrony. However, since also systemic oscillations decrease in power, the suppression of hemodynamic oscillations of

any kind could be critical to maintaining the neuronal synchrony in the first place. This hypothesis is supported by TCD evidence indicating that cerebral vasoreactivity is diminished in SWS.¹²⁹ In this case, then the transient hemodynamic changes in the SWS→LS transition might participate in stimulating neurons to end the synchronous behaviour.

The 1- and 4-cm signals exhibit parallel behaviour both during the sleep stage transitions and in the PSD analysis. However, there are notable qualitative differences between the 1- and 4-cm signals evident in the time domain (Fig. 6.4). Furthermore, we were able to demonstrate with PCA that the 4-cm signal averages in the sleep stage transitions. Together, these observations suggest that the changes in the 4-cm signals cannot be attributed to extracerebral contribution alone, and that there are considerable similarities in spontaneous hemodynamic behaviour between the scalp and the brain during sleep. Consequently, signal processing methods for removing extracerebral contribution that rely on the dissimilarities between scalp and cerebral circulation may be poorly suited for studies on spontaneous hemodynamics. Extending the source–detector separation and using more advanced light propagation models than MBLL (e.g., diffusion-equation-based modelling) may provide better approaches to dealing with extracerebral contribution in these cases.

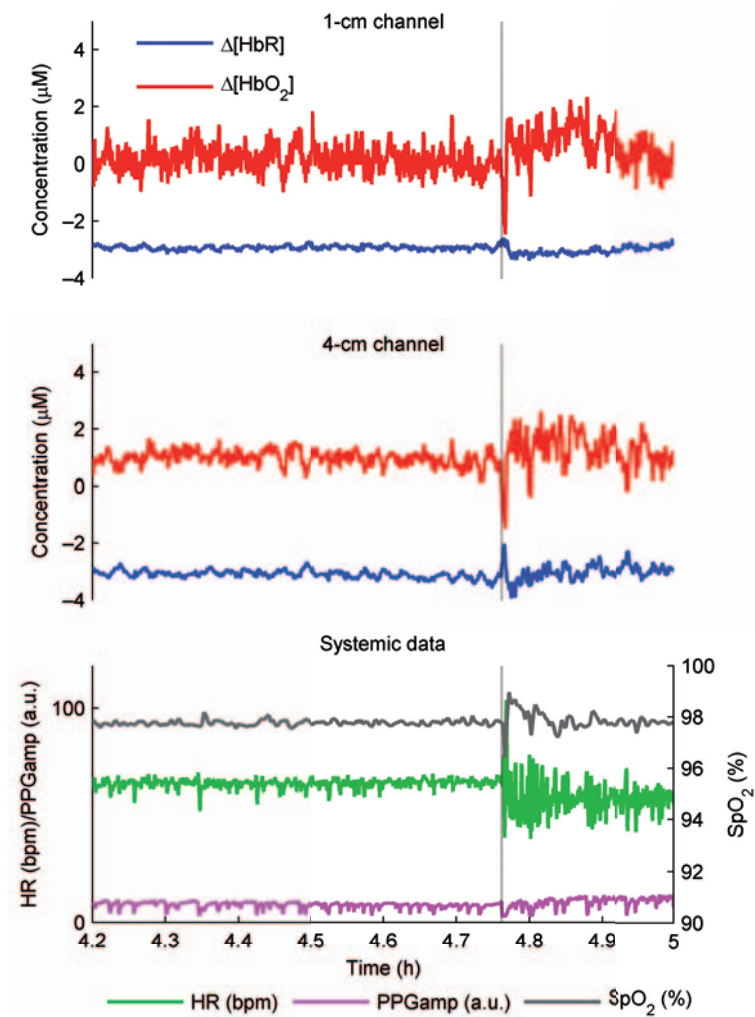


Figure 6.4. Evolution of $\Delta[\text{HbO}_2]$, $\Delta[\text{HbR}]$, HR, SpO_2 , and PPGamp during sleep in one representative subject. The vertical dotted line indicates a SWS→LS transition. The 4-cm signals exhibit an increase in hemodynamic fluctuations after the sleep stage transition that is not seen in the 1-cm signals. This behaviour can only be explained by the presence of a strong cerebral component in the 4-cm signals. (From Publication V.)

7. Conclusions and closing remarks

The monitoring studies presented in this thesis are the outcome of nearly ten years of NIRS methodology development at Aalto University. The results from previous pilot measurements allowed identifying and addressing crucial issues, such as motion artefacts in sleep measurements and extracerebral signal contribution during hypercapnia. The goal of this thesis was to develop methodology for NIRS monitoring of hypercapnia and sleep, and to provide references for physiological phenomena related to those conditions. For example, PCA was shown to be able to reduce extracerebral contribution to NIRS signals during various hypercapnic conditions. On the other hand, sometimes the cerebral signal can be so strong that there is no need to worry about extracerebral contribution, as was in the case of the breath hold measurements.

The analysis of breath hold responses provided new information on interindividual variation of cerebral and extracerebral hemodynamics both during and after end-expiratory breath hold. Finally, a novel method was introduced for correcting baseline motion artefacts in NIRS data. Applying this method to all-night NIRS measurements aided in the discovery of previously unknown features of sleep physiology. The central conclusions from these results can be summarised in three points:

1. Straightforward signal processing methods such as PCA are capable of removing extracerebral contribution from NIRS signals, but their use should be based on a case-by-case evaluation of their efficacy. For example, the 1-cm signal can be used as a reference for physiological noise in an evoked response study where it can be assumed that the neuronal response is statistically distinguishable from other hemodynamic changes. However, great care should be taken when interpreting results from a measurement where both extracerebral and cerebral hemodynam-

ics change in reaction to the same event. Forming a complete picture of the physiology of such events requires analysing also the scalp signals.

2. Studies on the hemodynamic response to sleep and hypercapnia would benefit greatly from a reference for typical variation in the response between subjects. For example, the results on apnea-induced cerebral hemodynamic changes in one OSA subject are different from the 'common pattern' reported in a previous NIRS study, but bear some resemblance to TCD results.^{23,97} Also, the analysis of end-expiratory breath hold responses in different subjects illustrates how key hemodynamic parameters such as HR may exhibit opposite behaviour in different subjects. Such references allow future investigators to better distinguish anomalies from normal variation.

3. Spontaneous hemodynamic oscillations are greatly reduced in SWS as opposed to LS and REM, and the SWS→LS and LS→REM transitions exhibit much more dramatic hemodynamic changes than the opposite transitions. Since this behaviour is seen in both the 1- and 4-cm channels, it appears to apply for both systemic and cerebral circulation, and there may even be some benefit from the simultaneous suppression of systemic and cerebral hemodynamic fluctuations related to the function of SWS.

The conclusions and experiences from this thesis pave the way for new measurement series, where the emphasis can shift from methodological development to addressing specific clinical and physiological questions related to monitoring applications. For example, measurements on a large population of OSA patients would allow establishing a reference for qualitative variation of the OSA response between individuals.

As NIRS studies tend to concentrate on hemodynamic changes related to neuronal activity, extracerebral changes are often either ignored or filtered away. This thesis shows that in monitoring applications of NIRS, acknowledging and studying the connections between cerebral and autonomic activity can provide valuable information of the functions and mechanisms of homeostatic regulation. The methodological improvements and new physiological observations presented here bring NIRS one step closer to a routine neurophysiological monitoring method in both clinical and research applications.

Bibliography

- [1] F. F. Jöbsis. Noninvasive, infrared monitoring of cerebral and myocardial oxygen sufficiency and circulatory parameters. *Science*, **198**:1264–1267, Dec. 1977.
- [2] Y. Hoshi. Functional near-infrared spectroscopy: Current status and future prospects. *Journal of Biomedical Optics*, **12**, 062106, Nov./Dec. 2007.
- [3] M. Wolf and G. Greisen. Advances in near-infrared spectroscopy to study the brain of the preterm and term neonate. *Clinics in Perinatology*, **36**:807–834, Dec. 2009.
- [4] T. Durduran, R. Choe, W. B. Baker, and A. G. Yodh. Diffuse optics for tissue monitoring and tomography. *Reports on Progress in Physics*, **73**:076701, Jul. 2010.
- [5] M. Wolf, M. Ferrari, and V. Quaresima. Progress of near-infrared spectroscopy and topography for brain and muscle clinical applications. *Journal of Biomedical Optics*, **12**, 062104, Nov./Dec. 2007.
- [6] J. M. Kane and D. M. Steinhorn. Lack of irrefutable validation does not negate clinical utility of near-infrared spectroscopy monitoring: Learning to trust new technology. *Journal of Critical Care*, **24**:472.e1–472.e7, 2009.
- [7] H. P. Grocott, S. Davie, and C. Fedorow. Monitoring of brain function in anesthesia and critical care. *Current Opinion in Anesthesiology*, **23**:759–764, 2010.
- [8] D. Highton, C. Elwell, and M. Smith. Noninvasive cerebral oximetry: is there light at the end of the tunnel? *Current Opinion in Anaesthesiology*, **23**:576–581, 2010.
- [9] C. Iadecola. Neurovascular regulation in the normal brain and in Alzheimer’s disease. *Nature Reviews Neuroscience*, **5**:347–360, May 2004.
- [10] I. Vanzetta and A. Grinvald. Coupling between neuronal activity and microcirculation: implications for functional brain imaging. *HFSP Journal*, **2**:79–98, Apr. 2008.
- [11] W. M. Ou, I. Nissilä, H. Radhakrishnan, D. A. Boas, M. S. Hämäläinen, and M. A. Franceschini. Study of neurovascular coupling in humans via simultaneous magnetoencephalography and diffuse optical imaging acquisition. *NeuroImage*, **46**:624–632, 2009.

- [12] H. Shibasaki. Human brain mapping: Hemodynamic response and electrophysiology. *Clinical Neurophysiology*, **119**:731–743, 2008.
- [13] M. E. Raichle and M. A. Mintun. Brain work and brain imaging. *Annual Review of Neuroscience*, **29**:449–476, 2006.
- [14] M. D. Fox and M. E. Raichle. Spontaneous fluctuations in brain activity observed with functional magnetic resonance imaging. *Nature Reviews Neuroscience*, **8**:700–711, 2007.
- [15] M. Massimini, G. Tononi, and R. Huber. Slow waves, synaptic plasticity and information processing: Insights from transcranial magnetic stimulation and high-density EEG experiments. *European Journal of Neuroscience*, **29**:1761–1770, 2009.
- [16] T. T. Dang-Vu, M. Schabus, M. Desseilles, V. Sterpenich, M. Bonjean, and P. Maquet. Functional neuroimaging insights into the physiology of human sleep. *SLEEP*, **33**:1589–1603, 2010.
- [17] D. A. Boas, A. M. Dale, and M. A. Franceschini. Diffuse optical imaging of brain activation: approaches to optimizing image sensitivity, resolution, and accuracy. *NeuroImage*, **23**:S275–S288, 2004.
- [18] T. J. Huppert, S. G. Diamond, M. A. Franceschini, and D. A. Boas. HomER: a review of time-series analysis methods for near-infrared spectroscopy of the brain. *Applied Optics*, **48**:D280–D298, 2009.
- [19] J. E. Brian. Carbon dioxide and the cerebral circulation. *Anesthesiology*, **88**:1365–1386, May 1998.
- [20] T. Przybyłowski, M.-F. Bangash, K. Reichmuth, B. J. Morgan, J. B. Skatrud, and J. A. Dempsey. Mechanisms of the cerebrovascular response to apnoea in humans. *Journal of Physiology*, **548**:323–332, 2003.
- [21] C. O. Olopade, E. Mensah, R. Gupta, D. Huo, D. L. Picchietti, E. Gratton, and A. Michalos. Noninvasive determination of brain tissue oxygenation during sleep in obstructive sleep apnea: a near-infrared spectroscopic approach. *Sleep*, **30**:1747–1755, 2007.
- [22] B. W. Carlson, V. J. Neelon, J. R. Carlson, M. Hartman, and S. Dogra. Cerebrovascular disease and patterns of cerebral oxygenation during sleep in elders. *Biological Research for Nursing*, **10**:307–317, 2009.
- [23] F. Pizza, M. Biallas, M. Wolf, E. Werth, and C. L. Bassetti. Nocturnal cerebral hemodynamics in snorers and in patients with obstructive sleep apnea: a near-infrared spectroscopy study. *SLEEP*, **33**:205–210, 2010.
- [24] J. C. G. Tsai. Neurological and neurobehavioral sequelae of obstructive sleep apnea. *NeuroRehabilitation*, **26**:85–94, 2010.
- [25] J. M. Krueger, D. M. Rector, S. Roy, H. P. A. Van Dongen, G. Belenky, and J. Panksepp. Sleep as a fundamental property of neuronal assemblies. *Nature Reviews Neuroscience*, **9**:910–919, 2008.
- [26] I. Nissilä, T. Noponen, J. Heino, T. Kajava, and T. Katila. Diffuse optical imaging. In J. Lin, editor, *Advances in Electromagnetic Fields in Living Systems*, volume 4: 77–130, Springer Science, 2005.

- [27] G. J. Tortora and S. R. Grabowski. *Principles of anatomy and physiology*. John Wiley & Sons, Inc., 9th edition, 2000.
- [28] T. J. Germon, P. D. Evans, A. R. Manara, N. J. Barnett, P. Wall, and R. J. Nelson. Sensitivity of near infrared spectroscopy to cerebral and extra-cerebral oxygenation changes is determined by emitter-detector separation. *Journal of Clinical Monitoring and Computing*, **14**:353–360, Jul. 1998.
- [29] T. Noponen. *Instrumentation for diffuse optical imaging and near-infrared spectroscopy and their applications in human brain studies*. Licentiate thesis. Helsinki University of Technology, Department of Engineering Physics and Mathematics, 2004.
- [30] M. Cope. *The application of near infrared spectroscopy to non invasive monitoring of cerebral oxygenation in the newborn infant*. Ph.D. thesis. University College of London, Department of Medical Physics and Bio-engineering, 1991.
- [31] A. Duncan, J. H. Meek, M. Clemence, C. E. Elwell, L. Tyszczyk, M. Cope, and D. T. Delpy. Optical pathlength measurements on adult head, calf and forearm and the head of the newborn infant using phase resolved optical spectroscopy. *Physics in Medicine and Biology*, **40**:295–304, 1995.
- [32] A. McGown, H. Makker, C. Elwell, P. G. Al Rawi, A. Valipour, and S. G. Spiro. Measurement of changes in cytochrome oxidase redox state during obstructive sleep apnea using near-infrared spectroscopy. *Sleep*, **26**:710–716, 2003.
- [33] S. J. Matcher, P. Kirkpatrick, K. Nahid, M. Cope, and D. T. Delpy. Absolute quantification methods in tissue near infrared spectroscopy. *Proceedings of SPIE*, **2389**:486–495, 1995.
- [34] V. Quaresima, S. Sacco, R. Totaro, and M. Ferrari. Noninvasive measurement of cerebral hemoglobin oxygen saturation using two near infrared spectroscopy approaches. *Journal of Biomedical Optics*, **5**:201–205, Apr. 2000.
- [35] G. Naulaers, B. Meyns, M. Miserez, V. Leunens, S. Van Huffel, P. Casaer, M. Weindling, and H. Devlieger. Use of tissue oxygenation index and fractional tissue oxygen extraction as non-invasive parameters for cerebral oxygenation. *Neonatology*, **92**:120–126, 2007.
- [36] G. W. Fischer and G. Silvay. Cerebral oximetry in cardiac and major vascular surgery. *HSR Proceedings in Intensive Care and Cardiovascular Anesthesia*, **2**:249–256, 2010.
- [37] D. T. Delpy, M. Cope, P. Vanderzee, S. Arridge, S. Wray, and J. Wyatt. Estimation of optical pathlength through tissue from direct time of flight measurement. *Physics in Medicine and Biology*, **33**:1433–1442, 1988.
- [38] R. Cubeddu, A. Pifferi, P. Taroni, A. Torricelli, and G. Valentini. Compact tissue oximeter based on dual-wavelength multichannel time-resolved reflectance. *Applied Optics*, **38**:3670–3680, 1999.

- [39] R. Re, D. Contini, M. Caffini, L. Spinelli, R. Cubeddu, and A. Torricelli. A compact time-resolved system for NIR spectroscopy. *Proceedings of SPIE*, **7368**:736815, 2009.
- [40] J. Selb, J. J. Stott, M. A. Franceschini, A. G. Sorensen, and D. A. Boas. Improved sensitivity to cerebral hemodynamics during brain activation with a time-gated optical system: analytical model and experimental validation. *Journal of Biomedical Optics*, **10**, 011013, Jan./Feb. 2005.
- [41] J. R. Lakowicz and K. Berndt. Frequency-domain measurements of photon migration in tissues. *Chemical Physics Letters*, **166**:246–252, 1990.
- [42] S. Fantini, M. A. Franceschini-Fantini, J. S. Maier, and S. A. Walker. Frequency domain multichannel optical detector for noninvasive tissue spectroscopy and oximetry. *Optical Engineering*, **34**:32–42, 1995.
- [43] S. Arridge, M. Cope, and D. T. Delpy. The theoretical basis for the determination of optical pathlengths in tissue: temporal and frequency analysis. *Physics in Medicine and Biology*, **37**:1531–1560, 1992.
- [44] M. A. Franceschini, S. Fantini, L. A. Paunescu, J. S. Maier, and E. Gratton. Influence of a superficial layer in the quantitative spectroscopic study of strongly scattering media. *Applied Optics*, **37**:7447–7458, 1998.
- [45] I. Nissilä, K. Kotilahti, K. Fallström, and T. Katila. Instrumentation for the accurate measurement of phase and amplitude in optical tomography. *Review of Scientific Instruments*, **73**:3306–3312, 2002.
- [46] I. Nissilä, T. Noponen, K. Kotilahti, T. Katila, L. Lipiäinen, T. Tarvainen, M. Schweiger, and S. Arridge. Instrumentation and calibration methods for the multichannel measurement of phase and amplitude in optical tomography. *Review of Scientific Instruments*, **76**, 044302, Apr. 2005.
- [47] Y. Hoshi, N. Kobayashi, and M. Tamura. Interpretation of near-infrared spectroscopy signals: A study with a newly developed perfused rat brain model. *Journal of Applied Physiology*, **90**:1657–1662, 2001.
- [48] L. P. Safonova, A. Michalos, U. Wolf, M. Wolf, D. M. Hueber, J. H. Choi, R. Gupta, C. Polzonetti, W. W. Mantulin, and E. Gratton. Age-correlated changes in cerebral hemodynamics assessed by near-infrared spectroscopy. *Archives of Gerontology and Geriatrics*, **39**:207–225, 2004.
- [49] L. A. Steiner and P. J. D. Andrews. Monitoring the injured brain: ICP and CBF. *British Journal of Anaesthesia*, **97**:26–38, 2006.
- [50] C. Iadecola and M. Nedergaard. Glial regulation of the cerebral microvasculature. *Nature Neuroscience*, **10**:1369–1376, Nov. 2007.
- [51] R. B. Buxton, K. Uludağ, D. J. Dubowitz, and T. T. Liu. Modeling the hemodynamic response to brain activation. *NeuroImage*, **23**:S220–S233, 2004.
- [52] F. Zheng, A. Sassaroli, and S. Fantini. Phasor representation of oxy- and deoxyhemoglobin concentrations: what is the meaning of out-of-phase oscillations as measured by near-infrared spectroscopy. *Journal of Biomedical Optics Letters*, **15**:040512, Jul./Aug.

- [53] X. Cui, S. Bray, and A. L. Reiss. Functional near infrared spectroscopy (NIRS) signal improvement based on negative correlation between oxygenated and deoxygenated hemoglobin dynamics. *NeuroImage*, **49**:3039–3046, 2010.
- [54] F. Scholkmann, S. Spichtig, T. Muehlemann, and M. Wolf. How to detect and reduce movement artifacts in near-infrared imaging using moving standard deviation and spline interpolation. *Physiological Measurement*, **31**:649–662, Mar. 2010.
- [55] M. Izzetoglu, P. Chitrapu, S. Bunce, and B. Onaral. Motion artifact cancellation in NIR spectroscopy using Kalman filtering. *BioMedical Engineering OnLine*, **9**:16, 2010.
- [56] I. Tachtsidis, C. E. Elwell, T. S. Leung, C.-W. Lee, M. Smith, and D. T. Delpy. Investigation of cerebral haemodynamics by near-infrared spectroscopy in young healthy volunteers reveals posture-dependent spontaneous oscillations. *Physiological Measurement*, **25**:437–445, 2004.
- [57] I. Schelkanova and V. Toronov. Optimal quantitation of the cerebral hemodynamic response in functional near-infrared spectroscopy. *Optics Express*, **18**:19386–19395, 2010.
- [58] J. M. Murkin, S. J. Adams, R. J. Novick, M. Quantz, D. Bainbridge, I. Iglesias, A. Cleland, B. Schaefer, B. Irwin, and S. Fox. Monitoring brain oxygen saturation during coronary bypass surgery: A randomized, prospective study. *Anesthesia and Analgesia*, **104**:51–58, Jan. 2007.
- [59] K. J. Cummings, M. Swart, and P. N. Ainslie. Morning attenuation in cerebrovascular CO₂ reactivity in healthy humans is associated with a lowered cerebral oxygenation and an augmented ventilatory response to CO₂. *Journal of Applied Physiology*, **102**:1891–1898, 2007.
- [60] L. Martin. *All you really need to know to interpret arterial blood gases*. Lippincott Williams & Wilkins, 2nd edition, 1999.
- [61] J. Urbano, V. Cruzado, J. López-Herce, J. del Castillo, J. M. Bellón, and Á. Carrillo. Optimal quantitation of the cerebral hemodynamic response in functional near-infrared spectroscopy. *Pediatric Pulmonology*, **45**:481–486, 2010.
- [62] T. Noponen, K. Kotilahti, I. Nissilä, T. Kajava, and P. Meriläinen. Effects of improper source coupling in frequency-domain near-infrared spectroscopy. *Physics in Medicine and Biology*, **55**:2941–2960, Apr. 2010.
- [63] J. Kerl, D. Köhler, and B. Schönhofer. The application of nasal and oronasal cannulas in the detection of respiratory disturbances during sleep: A review. *Somnologie*, **6**:169–172, 2002.
- [64] M. Folke, L. Cernerud, M. Ekström, and B. Hök. Critical review of non-invasive respiratory monitoring in medical care. *Medical and Biological Engineering and Computing*, **41**:377–383, 2003.
- [65] T. L. Lee-Chiong. Monitoring respiration during sleep. *Clinics in Chest Medicine*, **24**:297–306, 2003.

- [66] M. P. M. Harms. *Cerebral and cardiovascular dynamics in response to orthostatic stress*. Ph.D. thesis. University of Amsterdam, Faculty of Medicine, 2008.
- [67] S. Prince, V. Kolehmainen, J. P. Kaipio, M. A. Franceschini, D. Boas, and S. R. Arridge. Time-series estimation of biological factors in optical diffusion tomography. *Physics in Medicine and Biology*, **48**:1491–1504, Jun. 2003.
- [68] G. Morren, M. Wolf, P. Lemmerling, U. Wolf, J. H. Choi, E. Gratton, L. De Lathauwer, and S. Van Huffel. Detection of fast neuronal signals in the motor cortex from functional near infrared spectroscopy measurements using independent component analysis. *Medical & Biological Engineering & Computing*, **42**:92–99, Jan. 2004.
- [69] S. G. Diamond, T. J. Huppert, V. Kolehmainen, M. A. Franceschini, J. P. Kaipio, S.R. Arridge, and D. Boas. Dynamic physiological modeling for functional diffuse optical tomography. *NeuroImage*, **30**:88–101, Mar. 2006.
- [70] A. Akın and D. Bilensoy. Cerebrovascular reactivity to hypercapnia in migraine patients measured with near-infrared spectroscopy. *Brain Research*, **1107**:206–214, Aug. 2006.
- [71] I. Palada, A. Obad, D. Bakovic, Z. Valic, V. Ivancev, and Z. Dujic. Cerebral and peripheral hemodynamics and oxygenation during maximal dry breath-holds. *Respiratory Physiology & Neurobiology*, **157**:374–381, 2007.
- [72] C. Plathow, S. Ley, J. Zaporozhan, M. Schöbinger, E. Gruenig, M. Puderbach, M. Eichinger, H.-P. Meinzer, I. Zuna, and H.-U. Kauczor. Assessment of reproducibility and stability of different breath-hold maneuvers by dynamic MRI: Comparison between healthy adults and patients with pulmonary hypertension. *European Radiology*, **16**:173–179, 2006.
- [73] A. Rechtschaffen and A. Kales. *A manual of standardized terminology, techniques, and scoring system for sleep stages of human subjects*. Public Health Service, NIH Publication No. 204. US Government Printing Office, Washington, D.C., 1968.
- [74] C. Iber, editor. *The AASM manual for the scoring of sleep and associated events: Rules, terminology and technical specification*. American Academy of Sleep Medicine, 2007.
- [75] M. H. Silber, S. Ancoli-Israel, M. H. Bonnet, S. Chokroverty, M. M. Grigg-Damberger, M. Hirshkowitz, S. Kapen, S. A. Keenan, M. H. Kryger, T. Penzel, M. R. Pressman, and C. Iber. The visual scoring of sleep in adults. *Journal of Clinical Sleep Medicine*, **3**:121–131, 2007.
- [76] E. C.-P. Chua, S. J. Redmond, G. McDarby, and C. Heneghan. Towards using photo-plethysmogram amplitude to measure blood pressure during sleep. *Annals of Biomedical Engineering*, **38**:945–954, 2010.
- [77] Y. Hoshi, S. Mizukami, and M. Tamura. Dynamic features of hemodynamic and metabolic changes in the human brain during all-night sleep as revealed by near-infrared spectroscopy. *Brain Research*, **652**:257–262, 1994.

- [78] A. J. Spielman, G. Zhang, C. M. Yang, P. D'Ambrosio, S. Serizawa, M. Nagata, H. von Gizycki, and R. R. Alfano. Intracerebral hemodynamics probed by near infrared spectroscopy in the transition between wakefulness and sleep. *Brain Research*, **866**:313–325, Jun. 2000.
- [79] S. Shiotsuka, Y. Atsumi, S. Ogata, R. Yamamoto, M. Igawa, K. Takahashi, H. Hirasawa, K. Koyama, A. Maki, Y. Yamashita, H. Koizumi, and M. Toru. Cerebral blood volume in the sleep measured by near-infrared spectroscopy. *Psychiatry And Clinical Neurosciences*, **52**:172–173, 1998.
- [80] M. Igawa, Y. Atsumi, K. Takahashi, S. Shiotsuka, H. Hirasawa, R. Yamamoto, A. Maki, Y. Yamashita, and H. Koizumi. Activation of visual cortex in REM sleep measured by 24-channel NIRS imaging. *Psychiatry and Clinical Neurosciences*, **55**:187–188, 2001.
- [81] M. Uchida-Ota, N. Tanaka, H. Sato, and A. Maki. Intrinsic correlations of electroencephalography rhythms with cerebral hemodynamics during sleep transitions. *NeuroImage*, **42**:357–368, 2008.
- [82] J. Malmivuo and R. Plonsey. *Bioelectromagnetism, Principles and applications of bioelectric and biomagnetic fields*. Oxford University Press, 1995.
- [83] S. Kohno, I. Miyai, A. Seiyama, I. Oda, A. Ishikawa, S. Tsuneishi, T. Amita, and K. Shimizu. Removal of the skin blood flow artifact in functional near-infrared spectroscopic imaging data through independent component analysis. *Journal of Biomedical Optics*, **12**, 062111, Nov./Dec. 2007.
- [84] Q. Zhang, G. E. Strangman, and G. Ganis. Adaptive filtering to reduce global interference in non-invasive NIRS measures of brain activation: How well and when does it work? *NeuroImage*, **45**:788–794, 2009.
- [85] Q. Zhang, E. N. Brown, and G. E. Strangman. Adaptive filtering to reduce global interference in evoked brain activity detection: a human case study. *Journal of Biomedical Optics*, **12**, 064009, Nov./Dec. 2007.
- [86] A. Hyvärinen, J. Karhunen, and E. Oja. *Independent Component Analysis*. J. Wiley, 2001.
- [87] H. Zavala-Fernández, T. H. Sander, M. Burghoff, R. Orglmeister, and L. Trahms. Comparison of ICA algorithms for the isolation of biological artifacts in magnetoencephalography. *Lecture Notes in Computer Science*, **3889**:511–518, 2006.
- [88] M. Congedo, C. Gouy-Pailler, and C. Jutten. On the blind source separation of human electroencephalogram by approximate joint diagonalization of second order statistics. *Clinical Neurophysiology*, **119**:2677–2686, 2008.
- [89] V. D. Calhoun, J. Liu, and T. Adalı. A review of group ICA for fMRI data and ICA for joint inference of imaging, genetic, and ERP data. *NeuroImage*, **45**:S163–S172, 2009.
- [90] H. Mandelkow, D. Brandeis, and P. Boesiger. Good practices in EEG-MRI: The utility of *retrospective* synchronization and PCA for the removal of MRI gradient artefacts. *NeuroImage*, **49**:2287–2303, 2010.

- [91] D. S. Margulies, J. Böttger, X. Long, Y. Lv, C. Kelly, A. Schäfer, D. Goldhahn, A. Abbushi, M. P. Milham, G. Lohmann, and A. Villringer. Resting developments: A review of fMRI post-processing methodologies for spontaneous brain activity. *Magnetic Resonance Materials in Physics, Biology and Medicine*, **23**:289–307, 2010.
- [92] Y. H. Zhang, D. H. Brooks, M. A. Franceschini, and D. A. Boas. Eigenvector-based spatial filtering for reduction of physiological interference in diffuse optical imaging. *Journal of Biomedical Optics*, **10**, 011014, Jan./Feb. 2005.
- [93] C. B. Akgül, A. Akin, and B. Sankur. Extraction of cognitive activity-related waveforms from functional near-infrared spectroscopy signals. *Medical & Biological Engineering & Computing*, **44**:945–958, Nov. 2006.
- [94] J. Markham, B. White, B. Zeff, and J. Culver. Blind ICA discrimination of evoked cortical responses in humans with DOT. Organization for Human Brain Mapping 2008 Conference, Jun. 2008.
- [95] H. Zhang, Y.-J. Zhang, C.-M. Lu, S.-Y. Ma, Y.-F. Zang, and C.-Z. Zhu. Functional connectivity as revealed by independent component analysis of resting-state fNIRS measurements. *NeuroImage*, **51**:1150–1161, 2010.
- [96] T. Hayakawa, M. Terashima, Y. Kayukawa, T. Ohta, and T. Okada. Changes in cerebral oxygenation and hemodynamics during obstructive sleep apneas. *Chest*, **109**:916–921, Apr. 1996.
- [97] M. Furtner, M. Staudacher, B. Frauscher, E. Brandauer, M. M. Esnaola y Rojas, B. Gschliesser, W. Poewe, C. Schmidauer, M. Ritsch-Marte, and B. Högl. Cerebral vasoreactivity decreases overnight in severe obstructive sleep apnea syndrome: A study of cerebral hemodynamics. *Sleep Medicine*, **10**:875–881, 2009.
- [98] M. F. Bangash, A. Xie, J. B. Skatrud, K. J. Reichmuth, S. R. Barczi, and B. J. Morgan. Cerebrovascular response to arousal from NREM and REM sleep. *SLEEP*, **31**:321–327, 2008.
- [99] T. Wilcox, H. Bortfeld, R. Woods, and E. Wruck. Using near-infrared spectroscopy to assess neural activation during object processing in infants. *Journal of Biomedical Optics*, **10**:11010, Jan./Feb. 2005.
- [100] M. Izzetoglu, A. Devaraj, S. Bunce, and B. Onaral. Motion artifact cancellation in NIR spectroscopy using wiener filtering. *IEEE Transactions on Biomedical Engineering*, **52**:934–938, 2005.
- [101] P. N. Ainslie and J. Duffin. Integration of cerebrovascular CO₂ reactivity and chemoreflex control of breathing: Mechanisms of regulation, measurement, and interpretation. *American Journal of Physiology – Regulatory, Integrative and Comparative Physiology*, **296**:R1473–R1495, 2009.
- [102] W. Liboni, F. Molinari, G. Allais, O. Mana, E. Negri, G. bussone, G. D’Andrea, and C. Benedetto. Spectral changes of near-infrared spectroscopy signals in migraineurs with aura reveal an impaired carbon dioxide-regulatory mechanism. *Neurological Sciences*, **30**:S105–S107, 2009.

- [103] F. Molinari, W. Liboni, G. Grippi, and E. Negri. Relationship between oxygen supply and cerebral blood flow assessed by transcranial Doppler and near-infrared spectroscopy in healthy subjects during breath-holding. *Journal of NeuroEngineering and Rehabilitation*, **3**:16, 2006.
- [104] L. P. Safonova, A. Michalos, U. Wolf, J. H. Choi, M. Wolf, W. W. Mantulin, D. M. Hueber, and E. Gratton. Diminished cerebral circulatory autoregulation in obstructive sleep apnea investigated by near-infrared spectroscopy. *Sleep Research Online*, **5**:123–132, 2003.
- [105] M. Malik, J. T. Bigger, A. J. Camm, R. E. Kleiger, A. Malliani, J. Moss, and P. J. Schwartz. Heart rate variability: Standards of measurement, physiological interpretation, and clinical use. *European Heart Journal*, **17**:354–381, 1996.
- [106] G. W. Davis. Homeostatic control of neural activity: From phenomenology to molecular design. *Annual Review of Neuroscience*, **29**:307–323, 2006.
- [107] S. Vanhatalo, J. Voipio, and K. Kaila. Full-band EEG (FbEEG): An emerging standard in electroencephalography. *Clinical Neurophysiology*, **116**:1–8, 2005.
- [108] M. Burghoff, T. H. Sander, A. Schnabel, D. Drung, and L. Trahms. dc magnetoencephalography: Direct measurement in a magnetically extremely-well shielded room. *Applied Physics Letters*, **85**:6278–6280, 2004.
- [109] T. H. Sander, S. Leistner, H. Wabnitz, B.-M. Mackert, R. Macdonald, and L. Trahms. Cross-correlation of motor activity signals from dc-magnetoencephalography, near-infrared spectroscopy, and electromyography. *Computational Intelligence and Neuroscience*, **2010**:785279, 2010.
- [110] G. Zoccoli, A. M. Walker, P. Lenzi, and C. Franzini. The cerebral circulation during sleep: Regulation mechanisms and functional implications. *Sleep Medicine Reviews*, **6**:443–455, 2002.
- [111] P. Peigneux, G. Melchior, C. Schmidt, T. Dang-Vu, M. Boly, S. Laureys, and P. Maquet. Memory processing during sleep. mechanisms and evidence from neuroimaging studies. *Psychologica Belgica*, **44**:121–142, 2004.
- [112] L. Ayalon and S. Peterson. Functional central nervous system imaging in the investigation of obstructive sleep apnea. *Current Opinion in Pulmonary Medicine*, **13**:479–483, 2007.
- [113] M. Desseilles, T. Dang-Vu, M. Schabus, V. Sterpenich, P. Maquet, and S. Schwartz. Neuroimaging insights into the pathophysiology of sleep disorders. *SLEEP*, **31**:777–794, 2008.
- [114] T. T. Dang-Vu, M. Desseilles, S. Laureys, C. Degueldre, F. Perrin, C. Phillips, P. Maquet, and P. Peigneux. Cerebral correlates of delta waves during non-REM sleep revisited. *NeuroImage*, **28**:14–21, 2005.
- [115] M. Schabus, T. T. Dang-Vu, G. Albouy, E. Baletau, M. Boly, J. Carrier, A. Darsaud, C. Degueldre, M. Desseilles, S. Gais, C. Phillips, G. Rauchs, C. Schnakers, V. Sterpenich, G. Vandewalle, A. Luxen, and P. Maquet. Hemodynamic cerebral correlates of sleep spindles during human non-rapid eye movement sleep. *Proceedings of the National Academy of Sciences of the United States of America*, **104**:13164–13169, 2007.

- [116] T. T. Dang-Vu, M. Schabus, M. Desseilles, G. Albouy, M. Boly, A. Darsaud, S. Gais, G. Rauchs, V. Sterpenich, G. Vandewalle, J. Carrier, G. Moonen, E. Balteau, C. Degueldre, A. Luxen, C. Phillips, and P. Maquet. Spontaneous neural activity during human slow wave sleep. *Proceedings of the National Academy of Sciences of the United States of America*, **105**:15160–15165, 2008.
- [117] P. Maquet. Functional neuroimaging of normal human sleep by positron emission tomography. *Journal of Sleep Research*, **9**:207–231, 2000.
- [118] C. E. Elwell, R. Springlett, E. Hillman, and D. T. Delpy. Oscillations in cerebral haemodynamics. implications for functional activation studies. *Advances in Experimental Medicine and Biology*, **471**:57–65, 1999.
- [119] H. Obrig, M. Neufang, R. Wenzel, M. Kohl, C. Steinbrink, K. Einhäupl, and A. Villringer. Spontaneous low frequency oscillations of cerebral hemodynamics and metabolism in human adults. *NeuroImage*, **12**:623–639, 2000.
- [120] R. E. Haddock and C. E. Hill. Rhythmicity in arterial smooth muscle. *The Journal of Physiology*, **566**:645–656, 2005.
- [121] D. Linden and R. R. Diehl. Estimation of baroreflex sensitivity using transfer function analysis: normal values and theoretical considerations. *Clinical Autonomic Research*, **6**:157–161, 1996.
- [122] M. Valentini and G. Parati. Variables influencing heart rate. *Progress in Cardiovascular Diseases*, **52**:11–19, 2009.
- [123] H. Nilsson and C. Aalkjær. Vasomotion: Mechanisms and physiological importance. *Molecular Interventions*, **3**:79–89, 2003.
- [124] R. A. Weerakkody, M. Czosnyka, C. Zweifel, G. Castellani, P. Smielewski, N. Keong, C. Haubrich, J. Pickard, and Z. Czosnyka. Slow vasogenic fluctuations of intracranial pressure and cerebral near infrared spectroscopy – an observational study. *Acta Neurochirurgica*, **152**:1763–1769, 2010.
- [125] P. Bušek, J. Vaňková, J. Opavský, J. Salinger, and S. Nevšimalová. Spectral analysis of heart rate variability in sleep. *Physiological Research*, **54**:369–376, 2005.
- [126] B. Biswal, F. Z Yotkin, V. M. Haughton, and J. S. Hyde. Functional connectivity in the motor cortex of resting human brain using echo-planar MRI. *Magnetic Resonance in Medicine*, **34**:537–541, 1995.
- [127] V. Kiviniemi. Endogenous brain fluctuations and diagnostic imaging. *Human Brain Mapping*, **29**:810–817, 2008.
- [128] F. Amzica and M. Steriade. Electrophysiological correlates of sleep delta waves. *Electroencephalography and Clinical Neurophysiology*, **107**:69–83, 1998.
- [129] G. E. Meadows, D. M. O’Driscoll, A. K. Simonds, M. J. Morrell, and D. R. Corfield. Cerebral blood flow response to isocapnic hypoxia during slow-wave sleep and wakefulness. *Journal of Applied Physiology*, **97**:1343–1348, 2004.

Cover: Sleep and his half-brother Death by John William Waterhouse (1849-1917). In Greek mythology, Hypnos was the personification of sleep, son of the Goddess Nyx (night) and twin brother of Thánatos (death). The nature of sleep has fascinated man for thousands of years, yet we still know very little about its physiology. This thesis explores, among other things, the properties of cerebral circulation during human sleep. Image source: Julia Kerr <http://www.johnwilliamwaterhouse.com/> The image is in public domain.



ISBN 978-952-60-4231-2 (pdf)
ISBN 978-952-60-4230-5
ISSN-L 1799-4934
ISSN 1799-4942 (pdf)
ISSN 1799-4934

Aalto University
School of Science
Department of Biomedical Engineering and Computational Science

**BUSINESS +
ECONOMY**

**ART +
DESIGN +
ARCHITECTURE**

**SCIENCE +
TECHNOLOGY**

CROSSOVER

**DOCTORAL
DISSERTATIONS**